



João Miguel Coelho de Figueiredo

# PORTABLE SENSOR FOR EXPLOSIVES DETECTION

September 2016



UNIVERSIDADE DE COIMBRA





**FCTUC** FACULDADE DE CIENCIAS  
E TECNOLOGIA  
UNIVERSIDADE DE COIMBRA

Mestrado Integrado em Engenharia Electrotécnica e de Computadores

# Portable Sensor for Explosives Detection

João Miguel Coelho de Figueiredo

**Supervisor:**

Prof. Doutor Lino José Forte Marques

**Jury:**

Prof. Doutor Pedro Manuel Gens de Azevedo de Matos Faia

Prof. Doutor João Filipe de Castro Cardoso Ferreira

Prof. Doutor Lino José Forte Marques

Coimbra, September 2016



# Resumo

Resíduos de guerra ainda são um problema dos nossos dias. Uma das maiores preocupações em relação a este tópico são os campos minados ainda existentes e em localizações desconhecidas. Ainda no mês de Agosto do ano desta dissertação, a Organização Não Governamental (ONG) alertou jogadores Bósnios de um jogo baseado em localização GPS para que não entrassem em campos minados, após terem sido reportados alguns acidentes em campos de minas delimitados. Ainda hoje, com os conflitos no Médio Oriente, novos campos estão a ser preenchidos com minas.

Este problema tem vindo a ser estudado por várias entidades e projectos a nível mundial, de modo a ser possível identificar, remover e destruir minas de uma forma mais segura que a forma tradicional. Um destes projectos, e onde esta dissertação está incluída, é o *TIRAMISU*. O objectivo deste projecto, bem como o passo lógico a dar nesta área de estudo, consiste em usar a robótica e o que o mundo da tecnologia tem para oferecer, de modo a desenvolver novas formas de detectar explosivos, pois, com novas minas a serem construídas a partir de plásticos, a detecção comum usando detectores de metais está a tornar-se obsoleta.

O foco deste trabalho passa por construir uma nova solução para este problema, propondo um novo sensor que use vapores libertados por explosivos para identificar minas. Esta é uma temática com algum trabalho realizado que será explicado e utilizado ao longo desta dissertação.

Esta solução foi validada através de um trabalho experimental realizado com dados reais obtidos não por análise a minas, mas sim analisando soluções líquidas que simulam os referidos vapores. Os resultados obtidos foram promissores, provando que o conceito e configuração propostos podem ser usados para a detecção de minas.

**Palavras-chave:** Sensor, Perileno, Fluorescência, Nitroaromáticos, Minas



# Abstract

Remnants of war are still a real problem of our days. One of the main concerns related to this topic are the minefields still existent and of locations unknown. Even in August of the year of this dissertation, the Non-Governmental Organization (NGO) alerted Bosnian players of a location-based GPS game not to go into minefields, as there were some reports of recent accidents on marked mine zones. Even today, with the Middle Eastern conflicts, new fields are being filled with mines.

This problem has been studied by several entities and world projects in order to be able to identify, remove and dispose mines in a safer way than the traditional methods. One of this projects, and the one in which this dissertation is a part of is *TIRAMISU*. The goal of this project, and the logical step in this field of study, is to use robotics and what the world of technology has to offer, to develop new ways of sensing and detecting explosives, as with news mines being made out of plastic, the common detection by using a metal detector is becoming deprecated.

The focus of this work is to build a new solution for this problem by proposing a new sensor that uses vapors released by explosives into the air to identify mines. It is a theme with some background work that will be explained and used throughout this dissertation.

This solution was validated through experiments conducted over real data obtained not with by analyzing mines, but by analyzing liquid solutions that simulate said vapors. It has shown promising results, proving that the concept and configuration proposed can be used for detecting mines.

**Keywords:** Sensor, Perylene, Fluorescence, Nitroaromatics, Mines





# Acknowledgments

First I would like to express the deepest appreciation to my advisor, Prof. Doutor Lino Marques. Without his guidance and persistent help this dissertation would not have been possible.

To my family, and my girlfriend for all the support and patience that was always a constant throughout my years as a University student, which is a period in life that is not always easy.

And last but not least, I would like to thank all my friends, the ones that already were and the ones that came to be, for all help they gave me and the long dinners and nights. May they keep on happening throughout the years to come.



# Contents

<b>Resumo</b>	<b>iii</b>
<b>Abstract</b>	<b>v</b>
<b>Acknowledgments</b>	<b>vii</b>
<b>List of Acronyms</b>	<b>xi</b>
<b>1 Introduction</b>	<b>1</b>
1.1 TIRAMISU Project . . . . .	3
1.2 Objectives . . . . .	3
1.3 Document Overview . . . . .	4
<b>2 Sensors for Vapor-based detection of Explosives</b>	<b>5</b>
<b>3 Chemistry meets Physics through Electronics</b>	<b>9</b>
3.1 Aromatic Hydrocarbons . . . . .	9
3.1.1 Benzene . . . . .	10
3.1.2 Nitro Compounds . . . . .	10
3.1.3 Polycyclic Aromatic Hydrocarbons (PAHs) . . . . .	10
3.2 Luminescence . . . . .	11
3.2.1 Fluorescence . . . . .	13
3.3 Electronics . . . . .	14
3.3.1 Optoelectronics . . . . .	14
3.4 Overview . . . . .	17
<b>4 Sensor's Architecture</b>	<b>19</b>
4.1 Optical Conditioning . . . . .	19
4.1.1 Emitting and Referencing . . . . .	22

4.1.2	Emitting Fluorescence . . . . .	23
4.1.3	Detecting Fluorescence . . . . .	24
4.2	Signal Conditioning . . . . .	24
4.3	Processing . . . . .	25
4.3.1	Interface . . . . .	26
4.3.2	Communication Protocol . . . . .	26
4.4	Power Management . . . . .	29
4.5	Android Application . . . . .	30
4.6	Enclosure . . . . .	31
<b>5</b>	<b>Experimental Results</b>	<b>33</b>
5.1	Testing Table . . . . .	35
5.2	Testing Processes . . . . .	35
5.2.1	Test1 - Maximum Impurity . . . . .	36
5.2.2	Test2 - Impurity at a Controlled Flow Rate . . . . .	37
5.2.3	Test3 - Mixing Pure and Impure . . . . .	39
5.3	Response Analysis . . . . .	41
<b>6</b>	<b>Conclusion</b>	<b>45</b>
6.1	Future Work . . . . .	46

# List of Acronyms

<b>TIRAMISU</b>	Toolbox Implementation for Removal of Anti-personnel Mines, Sub-munitions and UXO
<b>UXO</b>	Unexploded ordnance
<b>ISR</b>	Institute of Systems and Robotics
<b>GPR</b>	Ground Penetrating radar
<b>LED</b>	Light Emitting Diode
<b>PAH</b>	Polycyclic Aromatic Hydrocarbon
<b>IUPAC</b>	International Union of Pure and Applied Chemistry
<b>TNT</b>	Trinitrotoluene
<b>PCB</b>	Printed Circuit Board
<b>DC</b>	Direct Current
<b>ADC</b>	Analog-to-Digital Converter
<b>PLL</b>	Phase-Locked-Loop
<b>UART</b>	Universal Asynchronous Receiver Transmitter
<b>USB</b>	Universal Serial Bus
<i>I<sup>2</sup>C</i>	Inter-Integrated Circuit
<b>MCCP</b>	Multiple Capture Compare Peripheral
<b>TTL</b>	Transistor-Transistor Logic
<b>FTDI</b>	Future Technology Devices International
<b>NEMA</b>	National Electrical Manufacturers Association
<b>DNB</b>	Dinitrobenzene
<b>DNT</b>	Dinitrotoluene
<b>TNT</b>	Trinitrotoluene
<b>DMNB</b>	Dimethyl-dinitrobutane



# List of Figures

1.1	Then and now maps from The Landmine Monitor [1]	2
2.1	Three-LED-based detection device [2].	6
2.2	Real testing unit and virtual internal architecture [3].	6
2.3	Differential approach on an optical sensor [4].	6
2.4	Diagram of the Oxygen Optode [5]	7
2.5	Diagram of the sensor's architecture [6]	7
2.6	Photograph of the sensor acquisition board [6]	7
2.7	FIDO X3 [7]	8
3.1	Benzene's Molecular Structure	10
3.2	Perylene's Molecular Structure	11
3.3	Jablonski Diagram	12
3.4	Perylene's Optical Properties [8]	13
3.5	LED Structure	15
3.6	Normalized Gaussian curves	15
3.7	Photodiode	16
4.1	Aluminum Optical Conditioning Chamber	20
4.2	Transmission percentage of incident light on EO 86-382 Dichroic Filter [9]	20
4.3	Excitation LED and Fluorescent Wavelengths	21
4.4	Schematic for Light Source PCB.	22
4.5	Perylene Films	23
4.6	Fluorescence Spectra with films in Ethylcellulose and ZEONEX	24
4.7	Differential approach for signal filtering	25
4.8	Communication Modules	26
4.9	Developed Android Application	30
4.10	Overview of the final product	31

5.1	Prepared solutions of DNB and DMNB . . . . .	34
5.2	Mass Flow Meter/Controller . . . . .	35
5.3	Test1 applied to ZEONEX and Ethylcellulose knife-coated films . . . . .	36
5.4	Test1 applied to ZEONEX and Ethylcellulose spin-coated films . . . . .	37
5.5	Test2 applied to ZEONEX and Ethylcellulose knife-coated films . . . . .	38
5.6	Test2 applied to ZEONEX and Ethylcellulose spin-coated films . . . . .	39
5.7	Test3 applied to ZEONEX and Ethylcellulose knife-coated films . . . . .	40
5.8	Test3 applied to ZEONEX and Ethylcellulose spin-coated films . . . . .	41
5.9	Interpolation of data set from Test3's procedure . . . . .	42
6.1	Overview of the final product . . . . .	45



# List of Tables

- 4.1 Available Command Codes for Communication with the Sensor . . . . . 27
- 4.2 Data available for each Command of Table 4.1 . . . . . 28
- 4.3 Forwarding to  $I^2C$  codes . . . . . 29



# Chapter 1

## Introduction

Antipersonnel mines are still a real threat and, in addition to the ones left by World War II, many mines are still being placed in some conflict regions, presenting newer problems like more sophisticated and “untraceable” mines, for example using different materials such as plastics instead of metal.

*“The United Nations is playing a vital role in freeing the world from the threat of mines and explosive remnants of war, meeting the needs of victims and survivors and ensuring their human rights. Last year alone, the United Nations destroyed more than 400,000 landmines and explosive remnants of war and more than 2,000 tons of obsolete ammunition. It cleared and verified more than 1,500 kilometers of roadways, provided mine risk education to millions of people and trained thousands of military and police officers to handle and safely dispose of explosive hazards.”* This was part of the message written by Ban Ki-moon, Secretary-General of the United Nations, on 4<sup>th</sup> of April last year, 2015, which is the International Day of Mine Awareness and Assistance in Mine Action. These accomplishments are, in a way, the result of the Mine Ban Treaty. This Treaty is officially called Convention on the Prohibition of the Use, Stockpiling, Production and Transfer of Anti-Personnel Mines and on their Destruction and was signed on the 18<sup>th</sup> of September of 1997. With this self explanatory title, it aims to *“put an end to the suffering and casualties caused by anti-personnel mines, that kill or maim hundreds of people every week, mostly innocent and defenseless civilians and especially children, obstruct economic development and reconstruction, inhibit the repatriation of refugees and internally displaced persons, and have other severe consequences for years after emplacement”* [10]. Basically it states that the parties involved cannot produce or develop anti-personnel mines, must destroy their stockpiles of anti-personnel mines within four years after signing and within ten years, all parties must have cleared all of their mined

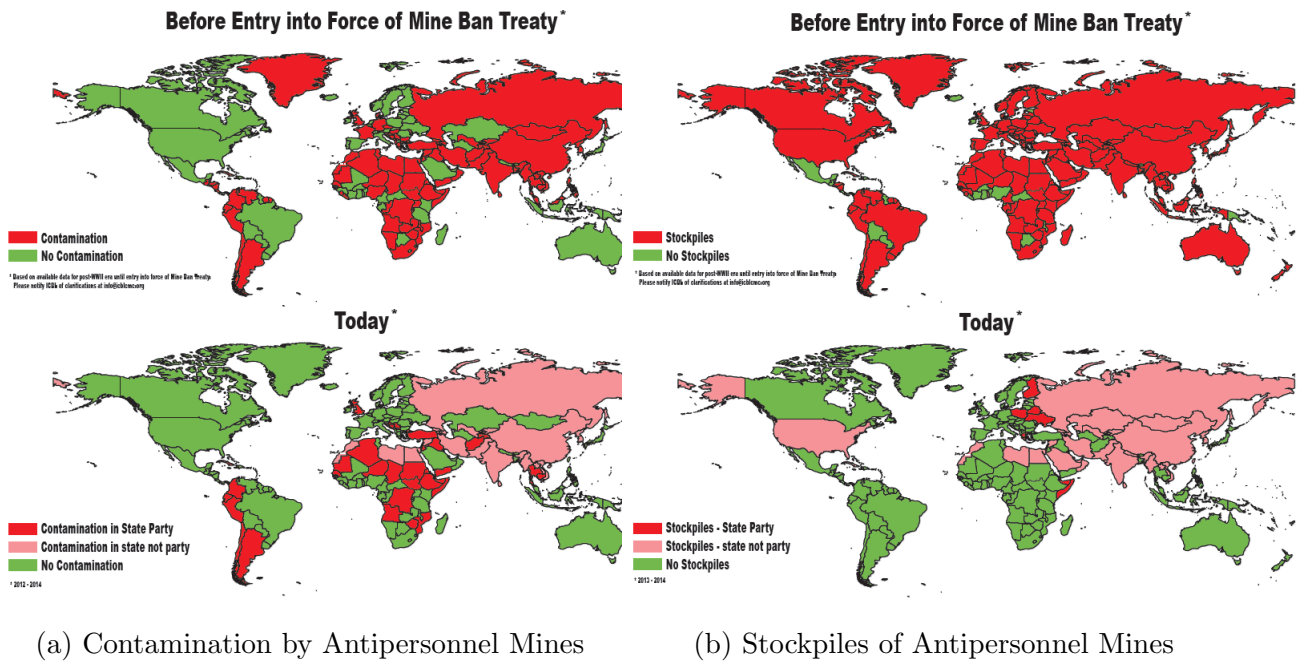


Figure 1.1: Then and now maps from The Landmine Monitor [1]

areas.

Figure 1.1, represents the comparison between before the treaty was in force and the year 2014. In terms of stockpiles it had a great result throughout the world eliminating a large percentage of the ones that existed before the treaty in the signing parties. The results in eliminating the contamination of landmines have also been very good but not as good due to the difficulty of finding unmarked minefields.

In the same message, Ban Ki-moon wrote *“Furthermore, civilians and communities are exposed to an increasingly wide range of explosive hazards, from mines to cluster munitions, unsafe and unsecured weapons and ammunition, and improvised explosive devices. I am extremely concerned by the extensive use of improvised explosive devices by armed groups in Iraq, which poses a major threat to civilians. In Syria, the widespread use of “barrel bombs” and other explosive weapons in populated areas has caused great devastation and human suffering, leaving a legacy of explosive remnants of war that will remain a threat until their removal.”* [11].

On top of this, the main topic of this thesis is also relevant in security scenarios like airports and border controls.

There are international projects promoting the development of new ways to identify and/or remove antipersonnel mines. This work is part of such a project, known as TIRAMISU.

## 1.1 TIRAMISU Project

The *Toolbox Implementation for Removal of Anti-personnel Mines, Sub-munitions and UXO*, TIRAMISU, is a project with the purpose of providing a toolbox to assist the Mine Action Community in addressing the many issues related to Humanitarian Demining, therefore promoting peace, national and regional security, conflict prevention, social and economic rehabilitation and post-conflict reconstruction. The tools developed are divided into three main categories:

- Demining management tools, which will help to locate landmines and UXOs, and define contaminated areas.
- Detection and disposal tools, which will neutralise mines and UXOs and safeguard the lives of operators.
- Training and Mine Risk education tools.

This work stands on the second category, being a tool to detect the mines through a specific method. The *Institute of Systems and Robotics* (ISR), located at the University of Coimbra, is responsible for two modules of this project and is the only Portuguese partner of TIRAMISU. These modules are “Stand-off detection” and “Ground-based Close-in Detection”. The first one’s purpose is to develop tools to detect explosives at medium to close range, using remotely controlled vehicles (aerial or ground-based). Ground-based Close-in Detection stands for the development of tools for close-range detection, as advanced metal detectors, Ground Penetrating Radars and chemical sensors.

## 1.2 Objectives

The main objective of this dissertation is to develop a portable solution, capable of detecting nitroaromatic compounds using fluorescent films.

With that said, this work can be divided into two main parts: development of electronics and an optical system that can detect said aromatics; and microcontroller programming to obtain a standalone smart sensor. The electronics can become very complex if one gets lost in the infinity of options in terms of technologies existent on the market and circuits to deliver similar results. One main objective through out this thesis is to keep things as simple as possible, while not compromising the results. The idea is to start simple and make it more complex as the need to do it presents itself along the way. The sensor in itself will

not be simple, but it shall be divisible into several modules, making it easier to comprehend. For the processing part, it was set from the beginning which technology to use. The goal and challenge in this part will be how to distribute and how to take maximum advantage of the modules present in this processing unit, while not compromising the responsiveness of the sensor in communicating with a master device as a computer or a tablet.

As described below in the Review of Literature (Chapter 2), there are some solutions for this detection problem. However, the ones that really deliver results tend to be too complex, as their objective is not just to detect one kind of vapors, but a vast range of them, which makes them very expensive. The study of how these detectors work is a good starting point for thinking and planning how to make a simpler and more focused kind of detector.

Overall, the question that this dissertation tries to answer is: How can explosives be detected in a simple yet effective, portable and not too expensive way?

### **1.3 Document Overview**

This dissertation starts out by giving a context on what has been and is being done in terms of explosives sensors, as well as sensors that use similar principles as the ones used during this project. Then it follows to a chapter describing some notions and concepts that give theoretical support to the solution proposed as sensor. The next chapter introduces the architecture of the sensor, explaining the different modules involved in it as well as the course of events that lead to a positive detection. At last the experimental results are presented, validating the final result, followed by some conclusions as well as suggestions for future work.

# Chapter 2

## Sensors for Vapor-based detection of Explosives

As stated before, still being a problematic of these days, there has been a great involvement around research and development of solutions for mine detection, deactivation and removal. This has led to various studies following different approaches to this problematic. Some approaches are based on metal detection or heat signatures or by analyzing data from ground penetrating electromagnetic waves generated by a technology called Ground Penetrating Radar (GPR). Another approach is to use optical based sensors. In addition to the work done in optical sensors specifically designed to address this explosives problematic, there are several works using similar base concepts for other purposes. In this dissertation both worlds will join to develop an optical sensor using fluorescence as its weapon to detect explosive materials.

With a simple search, one can find multiple articles and products using optical based sensors to detect concentrations of gases, like oxygen or carbon dioxide. There are several works with low complexity levels. One of them is a study by the University of Warsaw in Poland [2]. It is about a simple measurement system for photometric and fluorometric detection. The actual detection system consists in the usage of three LEDs where one is used as a light source and the other two are used as light detectors of limited bandwidth.

Another work, developed in the University of Idaho, in the United States of America, had as an objective, to build an explosives sensor, using Polycyclic Aromatic Hydrocarbons (PAHs) as well. It consisted of an integrating sphere with a tube inside. This tube was made out of a mixture of quartz and an explosive sensitive material. Part of this tube was covered with an optical fiber, leaving only a small portion exposed to the vapors [4]. Then,

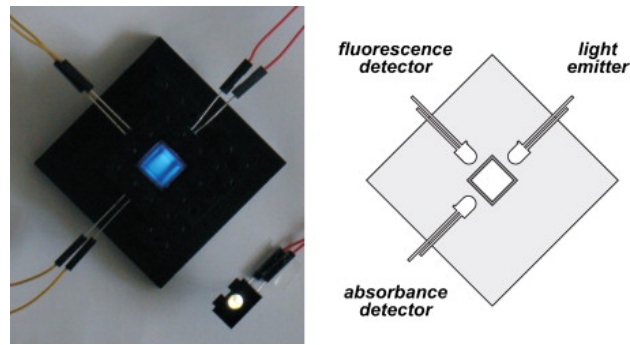


Figure 2.1: Three-LED-based detection device [2].

the quenching values were measured with a fluorimeter through the emission outlet port.

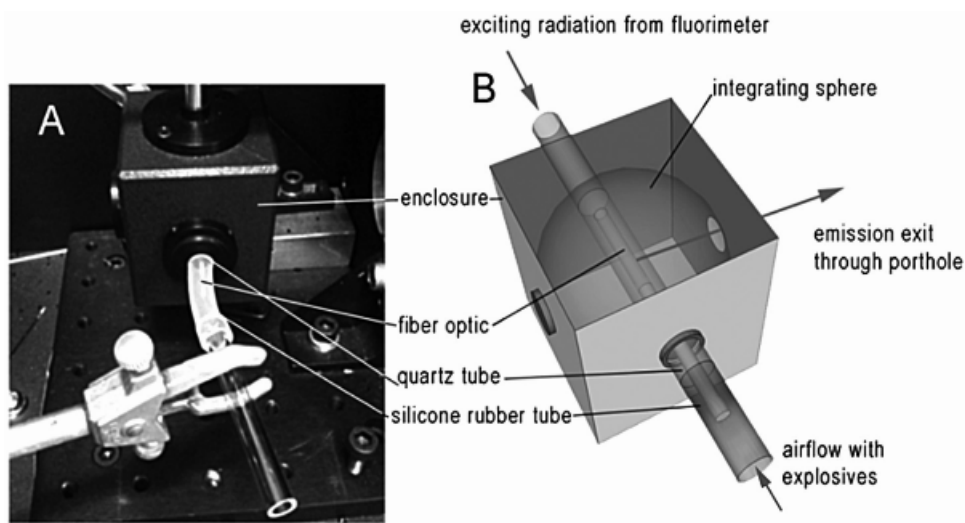


Figure 2.2: Real testing unit and virtual internal architecture [3].

This approach is not a portable solution. However, it is an interesting approach for the use of an integrating sphere which allows for a theoretical constant value of light intensity everywhere inside the sphere.

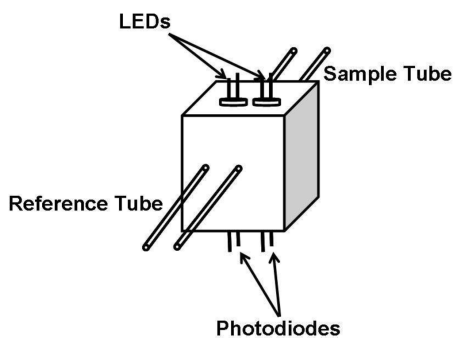


Figure 2.3: Differential approach on an optical sensor [4].

In terms of electronics, to measure quantities from the real world, one possible approach is to use a differential method, where there is a measurement of what is to be measured compared to another one called reference, in order to obtain a relative measure opposed to an absolute measure. This was made by a group of the University of Dublin. In Figure 2.3 is represented this differential approach, consisting of two tubes and two pairs LED-Photodiode, one coupled to the measurement tube, and the other to the reference tube. Being that it is, in fact,



a good approach, using two separate LEDs makes it insensible to fluctuations in the LEDs emissions, where, instead of stabilizing the measurement pair, the reference would produce “noise” creating fluctuations in the output signal.

One common application of fluorescence based optical sensors is the detection of oxygen. Aanderaa Instruments developed a sensor called “Oxygen Optode” which detects oxygen through luminescence quenching of a platinum porphyrins complex.

The oxygen measurement is made by a phase shift detection of the returning, oxygen quenched red luminescence [5]. After this detection, the relation between oxygen concentration and luminescent decay can be obtained through the Stern-Volmer equation. The film is excited using a green-blue light and the decay time is function of the phase of the received red light.

Prior to this work, another sensor was developed in the University of Coimbra to address the same problem.

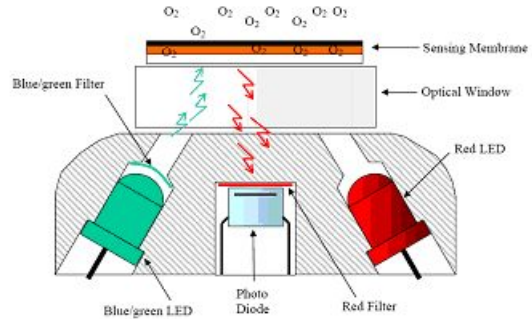


Figure 2.4: Diagram of the Oxygen Optode [5]

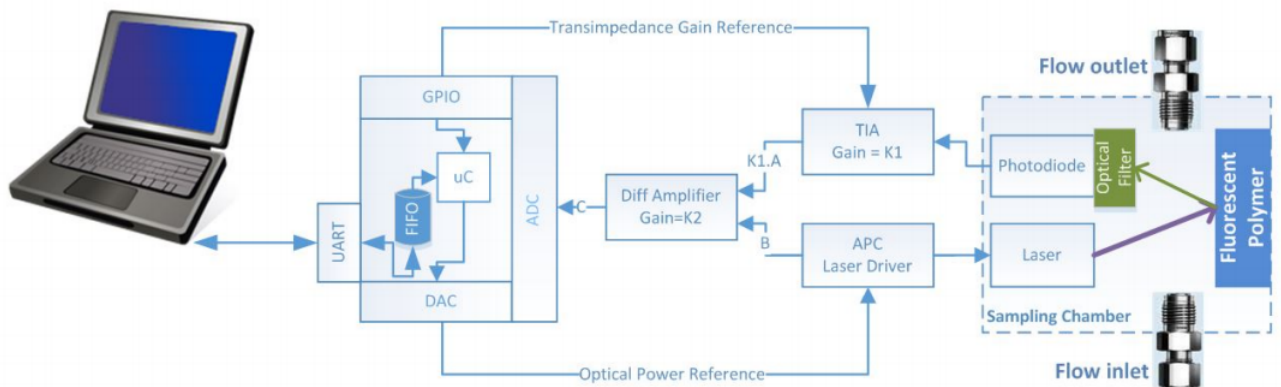


Figure 2.5: Diagram of the sensor’s architecture [6]

It consisted of an optical chamber with a laser LED and a photodiode both in the same surface of the chamber.



Figure 2.6: Photograph of the

The opposing surface was like a removable lid that allowed for a conjugated polymer to be deposited on it, thus using reflections of the laser to observe the fluorescence quenching with the photodiode with an

optical filter before it. The chamber also had a flow inlet and an outlet to circulate air inside of it. To retain from this is the use of a laser LED which has an internal photodiode for reference purposes.

The data would be acquired through a microcontroller which would then send it to a computer to be analyzed in MATLAB. Last but not least, there is a device available on the market made by the company FLIR. It is called FIDO X3 and the company claims it is the lightest and most sensitive handheld explosives trace detector in its class. They also claim this device evaluates if there is a threat or not in ten seconds.

It is a fluorescent based sensor as well. Analyzing the patent allows for a better understanding on how the sensor works [12]. It has got a sensitive part consisting of a fluorescent polymer, a light source, a photo detector and a signal converter. It is possible that the tube where the air flows is covered in the polymer allowing for a waveguide effect in the polymer's structure producing high intensities of fluorescence and great exposure of the polymer to the vapors.

Despite this being an excellent product with very high sensitivity and a large range of substances it can detect, plastic mines present a problem for they have a very low concentration of vapors, that are easily confused with noise by the X3 device.



Figure 2.7: FIDO X3 [7]

# Chapter 3

## Chemistry meets Physics through Electronics

### 3.1 Aromatic Hydrocarbons

Hydrocarbons are compounds of carbon and hydrogen and represent one of the most significant classes of organic compounds. Though they play a major role in chemistry, industrial applications have been diminishing their usage, mainly for environmental concerns that lead to new regulatory problems.

The International Union of Pure and Applied Chemistry (IUPAC) Nomenclature of Organic Chemistry divides hydrocarbons in four main types [13]:

- Saturated hydrocarbons(alkanes);
- Unsaturated hydrocarbons(alkenes and alkynes);
- Cycloalkanes;
- Aromatic hydrocarbons(arenes);

This last type gets its name because many of the hydrocarbons classified as aromatic present a sweet and/or pleasant odor. The simplest aromatic hydrocarbon is Benzene which will be explored below.

### 3.1.1 Benzene

As said, benzene is an organic chemical compound of the group of aromatic hydrocarbons. Its chemical formula is  $C_6H_6$  and its molecular structure is represented in Figure 3.1. It has a sweet almond like odor and is highly flammable.

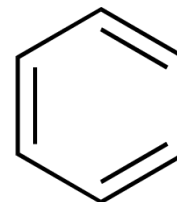


Figure 3.1: Benzene's Molecular Structure

This compound can be obtained from natural sources (volcanoes, forest fires, as a part of crude oil, ...), or from other human activities. It is used to make, for example, plastics, resins, dyes, lubricants and drugs. In the United States of America, it ranks in the top 20 most produced chemicals [14].

### 3.1.2 Nitro Compounds

Nitro compounds are organic compounds that contain one or more nitro ( $NO_2$ ) functional groups. The nitro functional groups are what turns a substance explosive. The higher the number of nitro functional groups present, the more unstable and, therefore, more explosive the substance is. For instance, TNT, the known explosive, stands for trinitrotoluene ( $C_6H_2(NO_2)_3CH_3$ ), which is composed of toluene (aromatic hydrocarbon) with three nitro groups that make it highly explosive, or nitroglycerin that is highly explosive as well, due to the presence of a nitro group. The majority of landmines and other explosives in general use TNT as their explosive compound. For this reason, in this work, vapors from the nitro compounds nitrobenzene and dinitrobenzene, which resemble the chemical composition of landmines, were used as testing environment for the sensor.

### 3.1.3 Polycyclic Aromatic Hydrocarbons (PAHs)

The term Polycyclic Aromatic Hydrocarbons refers to a group of chemically-related and environmentally persistent organic compounds of various structures and toxicities. They get this name for their molecular structure which has two or more, single or fused aromatic rings, with a pair of carbon atoms between rings. In particular, PAH refers to compounds consisting of carbon and hydrogen atoms only. The main characteristics of PAHs are:

- High melting and boiling points;
- Low vapor, pressure and aqueous solubility;
- Soluble in various organic solvents.

The major source of PAHs is the incomplete combustion of organic materials such as coal, oil and wood. They are mostly used in pharmaceuticals, agriculture, photographic products, lubricators and other chemical industries. Specific refined PAHs can also be used in the field of electronics, and liquid crystals.

The main route of exposure to PAHs is from breathing, eating food containing PAHs, smoking cigarettes or breathing smoke. Many PAHs are known or suspected to be a human carcinogen. For non-smokers, the main carrier for PAHs is food. When various types of meat, as beef, pork, fish or poultry, are cooked with high temperature, PAHs are formed and, since these hydrocarbons have been found to be mutagenic, eating these kinds of meat cooked, for example, over an open flame, can increase the risk of cancer. More information on this matter can be found in the “Toxicological Profile for Polycyclic Aromatic Hydrocarbons” from the U.S. Department of Health and Human Services [15].

### Perylene

The Polycyclic Aromatic Hydrocarbon used in this work is the perylene. This substance is not classifiable as to its carcinogenicity to humans [15], but it is, nonetheless, considered to be a hazardous pollutant. However, in this work, perylene is used in solid state as part of a thin film and does not release vapors and, therefore, is not dangerous.

Perylene’s chemical formula is  $C_{20}H_{12}$  and its molecular structure is represented in Figure 3.2. In many cases, such as in this work, perylene is used for its fluorescent properties. Later in this document, this properties will be explored, as they are an essential part of this work.

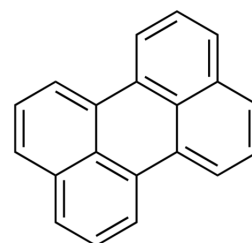


Figure 3.2: Perylene’s Molecular Structure

## 3.2 Luminescence

Luminescence is the phenomenon by which a substance emits electromagnetic waves through the form of light. This phenomenon does not result from heat and, therefore, is not to be confused with incandescence. Luminescence can be caused by chemical reactions, electrical energy, subatomic motions or stress on a crystal . There are several types of luminescence. Some of them are listed bellow:

- Chemiluminescence - result of chemical reaction;

- Electroluminescence - result of passing electric current;
- Mechanoluminescence - result of mechanical action on a solid;
- Photoluminescence - result of absorption of photons;
- Radioluminescence - result of bombardment by ionizing radiation

Photoluminescence is, as said, a phenomenon of luminescence characterized by the absorption of photons that excite the molecules in a given substance and then, during their relaxation processes, re-radiate other photons.

This phenomenon can be divided into two other phenomena: fluorescence and phosphorescence. The main difference between them in terms of visualization is that the latter is a much slower process while the former is an almost instantaneous process.

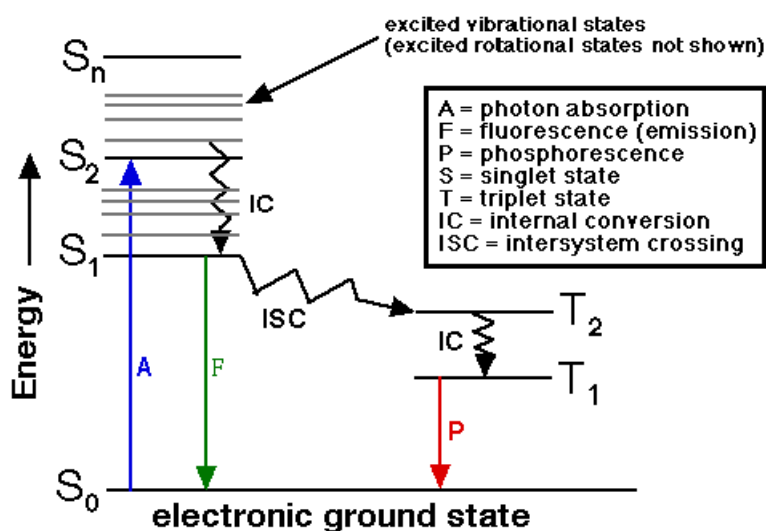


Figure 3.3: Jablonski Diagram

The Figure 3.3 is known as Jablonski Diagram and illustrates the electronic states of a molecule and the transitions between them.

In physical terms, phosphorescence occurs when photons undergo intersystem crossing where they enter a state with altered spin multiplicity. When entering the triplet state, the transition to lower singlet energy states is quantum mechanically forbidden, which means it will occur much slowly, lasting up to hours. This is the basic principal of “glow in the dark” substances. Fluorescence, on the other hand, is a very fast process in which photon absorption occurs with some loss of energy. As a result, when molecules re-transition to their original state, the released photons will have lower energy than the original ones. This is called a red shift, due to red being the less energetic primary color in the visible spectrum.

### 3.2.1 Fluorescence

Among the various types of luminescence explained above, the one this work is interested in is Fluorescence. This is where things start to connect and where Chemistry meets Physics. We have discussed several chemical compounds and physics phenomena. The key for this entire work is the existence of a substance (perylene) than can be arranged in a thin film form, in such a way that it can be excited into showing high fluorescent intensity that can be decreased in the presence of nitro compounds such as the ones used to make explosive charges like nitrobenzene. This arrives to question asked in the Introduction of this document: How can explosives be detected in a simple yet effective, portable and not too expensive way?

As known and explained above, when fluorescence occurs, the emitted light is of a lower level of energy and thus a higher wavelength than the received light, responsible for the molecules' excitation. In a perfect system/environment, the fluorescent film would absorb 100% of the excitation light so that, after the film, the existing light would only be fluorescence-based light. This is very difficult to achieve and because of that, certain things have to be taken into consideration.

As said in a subsection above, perylene is mostly used for its fluorescent properties. In Figure 3.4, are represented perylene's optical absorption and emission spectra.

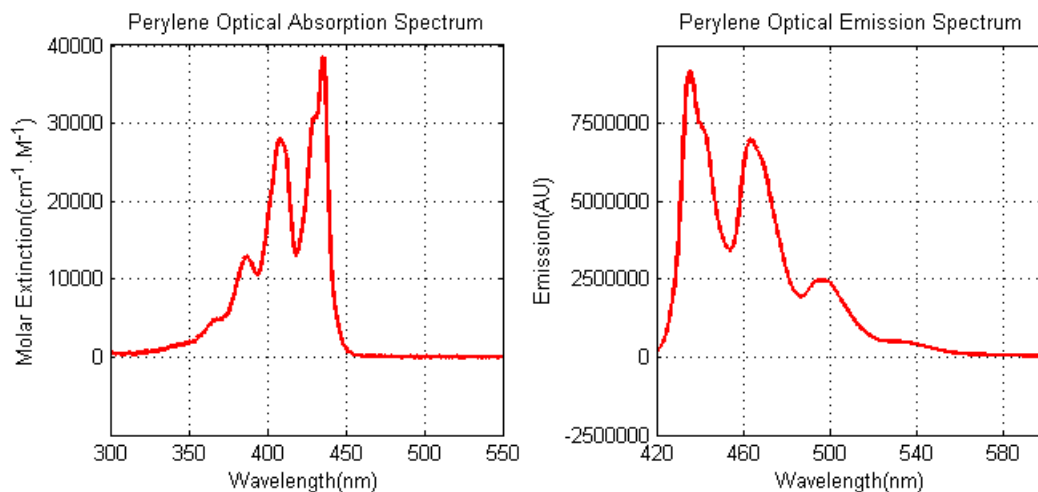


Figure 3.4: Perylene's Optical Properties [8]

By analyzing the above spectra and its data through a MATLAB script, it can be concluded that this PAH has, essentially, two relative maxims in terms of absorption: 408nm and 435nm. As for fluorescence intensity levels, it shows relative maxims at 435nm, 463nm, and 496nm.

The focus should be on well separated wavelengths, so that they can be well filtered

through optical filters. This way, the wavelength that has been chosen for light source will be around the 408nm and the wavelength resulting from the fluorescence will be around the 463nm.

### 3.3 Electronics

Electronics is the science that studies ways to manipulate electricity through the usage of active and passive electrical components that, when together and arranged in such a manner that produce some kind of desired output, are called electronic circuits. This science has been evolving exponentially since the first radio transmissions in 1895 by Marconi, followed by many great discoveries like the transistor or the low-loss optical fiber.

In general, electronics can be divided into two main cores: Analog and Digital. Usually, when working with electronics, one uses both worlds connecting them, as will happen and therefore will be explained in this project. Simply put, digital electronics process information and or signals in a binary form (in terms of 1s and 0s), so there are only two levels of amplitude that a signal can take (High and Low). On the other hand, most of the physical world is analog. For instance, our senses represent variables such as vision and smell in an analog manner. Here enters the world of transducers and sensors. A sensor, and specifically a smart sensor, is a device capable of analyzing analog data from the “real” world and transforming it into either readable and intelligible data for the human user or an action, like a thermometer converting heat into numbers that are readable and have some meaning or a motion sensor that opens a door.

#### 3.3.1 Optoelectronics

In a more specific part of electronics, there is optoelectronics that uses and studies electronics to, essentially, emit, control and detect light. Optoelectronics is often considered a sub-field of photonics that are the actual science studying all aspects of light at photon level, like, how to generate detect and manipulate light through emission, transmission, modulation, signal processing, switching, amplification, and detection. This studies are both crucial to this work.



## LED

Light Emitting Diodes (LED) have been around for a while now. They have been used in a large specter of uses, whether it is for industrial purposes, “debugging” situations, illumination or even just design and beauty applications.

LEDs are a p-n junction diode that emit light when a certain voltage is applied to their leads. The n-layer is a layer doped with electrons where p-layer is a layer injected with holes. Applying a forward voltage to the LED will cause an electron-hole recombination which will have energy losses resulting in the release of photons. There is also a type of loss resulting from electron-hole recombination that will not produce light, but heat instead.

Nowadays, LED manufacturers can achieve almost every color in the visible spectrum by using different materials and compositions as a semiconductor. The characteristic curve of emission of an LED behaves more or less like a Gaussian function:

$$f(x) = ae^{-\frac{(x-b)^2}{2c^2}} \quad (3.1)$$

In the above expression 3.1,  $a = \frac{1}{\sigma\sqrt{2\pi}}$ ,  $b = \mu$  and  $c = \sigma$ , following the pattern in the bellow Figure 3.6.

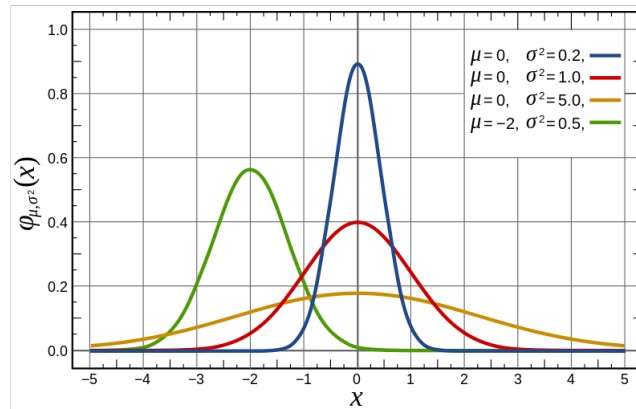


Figure 3.6: Normalized Gaussian curves

The value  $\mu$  is called expected value and, in the case of led emission spectrum it is equivalent to the main wavelength emitted by it. There is also another important value in Gaussian functions which is the variance,  $\sigma^2$ , a value used in statistics equivalent to the square of standard deviation. For LEDs, this value represents the range of wavelengths it

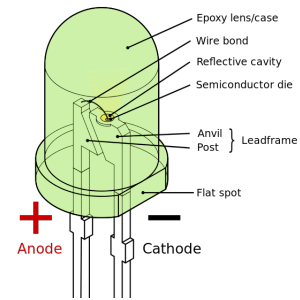


Figure 3.5: LED Structure

emits. As said before, this type of diodes achieve certain colors by using specific materials in their composition. However, there can be some fluctuations in  $\mu$  and  $\sigma$  values due to the temperature in the p-n junction [19]. With temperature increase, wavelength emitted by the LED will tend to increase as well, which is known as a “red shift”. Along with this, the variance value,  $\sigma^2$ , will tend to decrease, resulting in a broader band of emitted wavelengths.

A great breakthrough in the development of LEDs was the discovering of how to make a white LED. This is also a breakthrough for illumination, as these diodes are much more efficient (electrically speaking) than, for example, the incandescent light bulbs. White LEDs are the combination of blue LEDs and the principle of fluorescence (described in Section 3.2.1). Using some phosphors in the coating of the LED, the best white led is achieved using fluorescence to obtain red and green lights from the blue one, in such a way that the mixing of this colors is perceived as white. Another way white color can be achieved is by adding some yellow to the blue. The latter has the problem that green and red objects are not well illuminated.

## Photodiode

A photodiode is the inverse of an LED. As well as the light emitter, it is also a semiconductor device, but instead of emitting light, it absorbs it and converts it into electrical current. It is, therefore, a device that converts light into an electrical signal. In order to increase response times, many photodiodes use a PIN junction instead of p-n junction. Much like the p-n junction, it has two layers doped with electrons and holes but, between them, it has a an undoped layer, called intrinsic semiconductor region.

When a photon reaches the surface of the semiconductor, its energy is absorbed. This creates, if the photon has enough energy, a rearrangement of the hole-electron pairs. In the undoped region, these pairs are balanced, i.e., for every electron there is a hole and vice versa. In order to stay this way, when the photon’s energy is absorbed holes move towards the anode and electrons towards the cathode, thus producing current, designated as photocurrent. The total current produced by a photodiode is the sum of the photocurrent produced by the intensity of light absorbed and a type of current known as dark current [20]. Dark current can be seen as a form of noise or parasite current that is generated in the absence of light, for instance, by background radiation.



Figure 3.7: Photodiode

## 3.4 Overview

In this chapter all main aspects related to this work were discussed, reaching a starting point to answer the question asked in Section 3.2.1: How can explosives be detected in a simple yet effective, portable and not too expensive way?

The perylene film produces fluorescent light when excited by radiation of a specific wavelength. Using LED technology, this specific wavelength can easily be emitted to the film and photodiodes can be used to retrieve information about fluorescence intensity levels. Knowing that the fluorescence levels of perylene are attenuated by the presence of nitro compounds such as the ones present in explosives, with some additional electronics such as microcontrollers and amplifiers, a new method for explosive detection should be possible.



# Chapter 4

## Sensor's Architecture

Having mentioned and explained all crucial materials and elements of the project in the previous chapter, here the sensor itself will be discussed part by part.

It consists essentially of three parts:

- Optical conditioning;
- Signal conditioning;
- Processing unit.

All of these parts will be explained in detail further in this chapter. Generally speaking, the sensor consists of a shielded module that can operate in standalone mode or by communicating with a computer or another device through serial communication or Bluetooth. It also employs a feature of forwarding messages not directed to it into an  $I^2C$  bus line. This bus line will be accessible allowing the addition of  $I^2C$  based devices and/or sensors like, for instance, a MOX sensor.

### 4.1 Optical Conditioning

At the beginning of this project, there was the need to assess what existed and had been made to address this same problem. Previous solutions based their optical conditioning in the maximization of multiple reflections in a polymer using a focused laser beam. The objective was to design a chamber based on an integrating sphere. This solution had various problems like how to easily change the film or even how to make a film that would adhere to the interior surface of the chamber. Another problem with this approach is the optical power

of the laser that would burn the polymer over time, decreasing its fluorescent properties and, ultimately, making the polymer unusable.

On a more direct approach, the design chosen for this work is a chamber made of aluminum with a cylindrical hole inside and the film essentially dividing this hole into two.

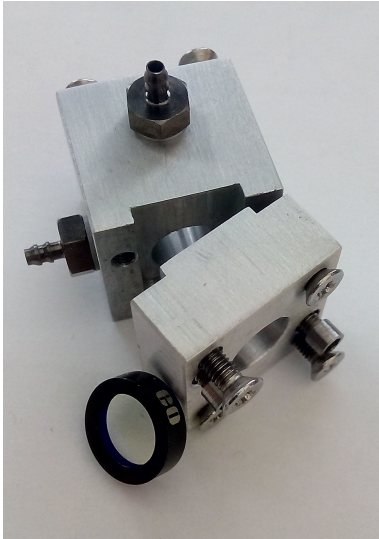


Figure 4.1: Aluminum Optical Conditioning Chamber

In Figure 4.1 is the aluminum chamber designed and constructed. It has two threaded holes on the bottom side that are for mounting purposes. The interior cavity has 9mm of diameter that was designed to match the optical filter's clear aperture. The optical filter had to be chosen taking into account the need to filter the emission light, eliminating (or reducing) its presence before it could reach the photodiode's sensitive area. The chosen filter (in the Figure 4.1) was, therefore, the Edmund Optics 86-382. This filter is of the Dichroic type, which is a color filter that allows light of a range of colors pass while reflecting the others. In the case of this filter, it reflects wavelengths between 372 - 415 nm, transmitting between 439 - 647.1 nm, having a reflection percentage of more than 98%, while

the transmission is more than 95% of the incident light [9]. These values are shown in the below diagram, Figure 4.2 which is part of the official Edmund Optics datasheet of said filter:

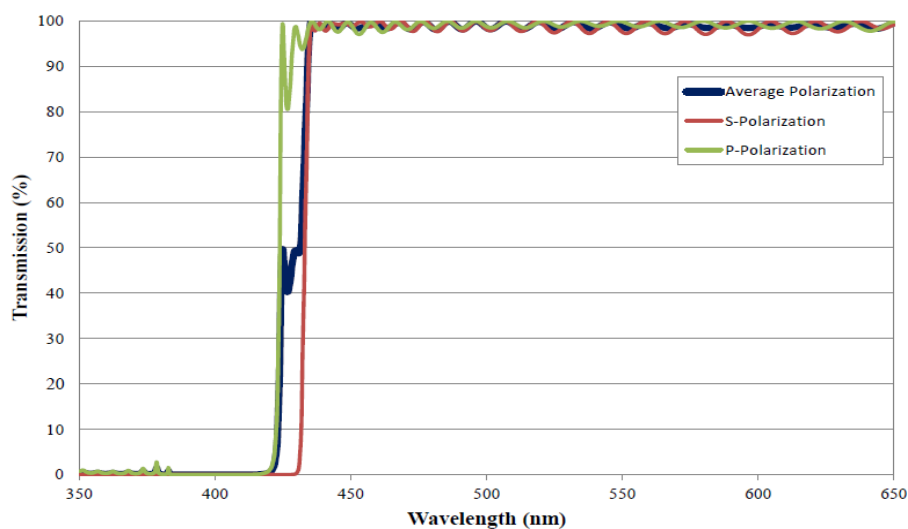


Figure 4.2: Transmission percentage of incident light on EO 86-382 Dichroic Filter [9]

In Figure 4.1 it is also visible that the chamber is actually built in two pieces. It

was made this way to accommodate a very thin slot where the film will easily be placed and removed. As said before, this film will essentially divide the chamber in two. On one side (smallest piece) will be the emission part with the proper LED. On the other one will be the photosensitive part of the sensor with the photodiode and the optical filter before it. Aside from this parts, the chamber also has got two holes that work as inlet and outlet for the air that will pass through the chamber.

To work properly, the chamber has to be isolated from outside light sources, so it has four threaded holes on each side of the interior cavity. This way two lids can be screwed in isolating it. Two PCBs(Printed Circuit Board) are used as lids, one with the circuit for driving the LED and another one for the photodiode and respective signal conditioning. The interior cavity has also been polished to allow for better reflections inside of it.

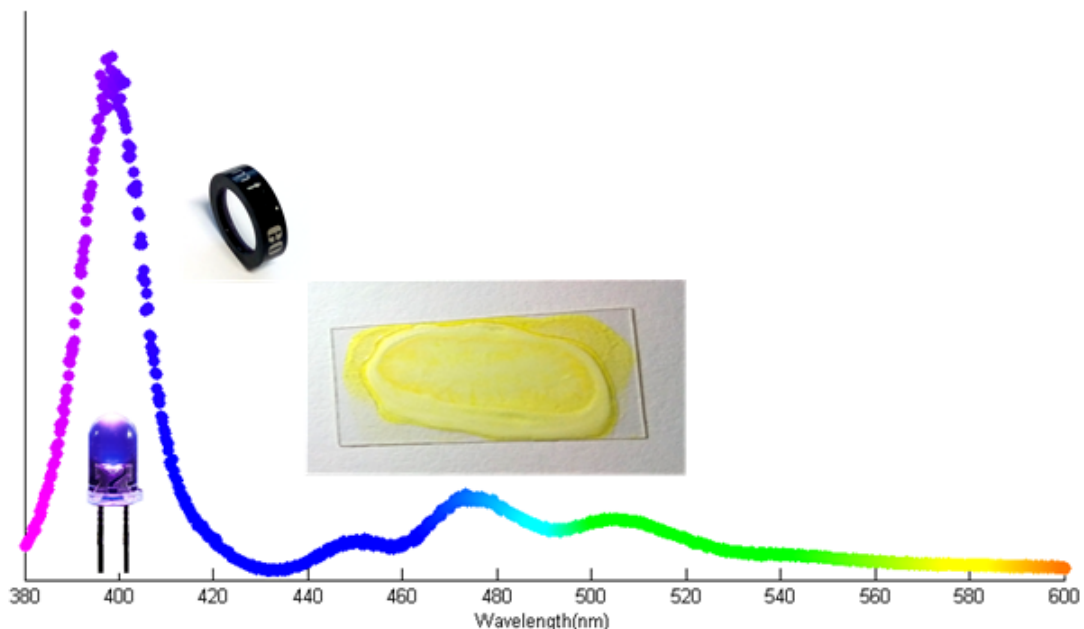


Figure 4.3: Excitation LED and Fluorescent Wavelengths

In terms of spectra, the above image (Figure 4.3), shows the visible part of the electromagnetic spectrum, positioning the different parts of the optical chamber where they sit in it. This spectrum was captured using The USB4000 spectrometer from Ocean Optics and plotted through MATLAB using a converter algorithm to correlate the points' colors in RGB with the associated wavelengths in the spectrum. Around the 405nm is the excitation LED production the photons that will excite the molecules in the film (at the right) into fluorescent-making energy levels, while at the middle, the filter will cut all wavelengths below 427nm, allowing only fluorescent light to reach the photosensitive device.

### 4.1.1 Emitting and Referencing

As said before, the chamber has got two PCBs attached to their extremities, making immune to outside light. One of the PCBs has the components responsible for light emitting and creating a reference signal with a photodiode coupled to the excitation light emitting diode. In Figure 4.4 is the schematic for this board.

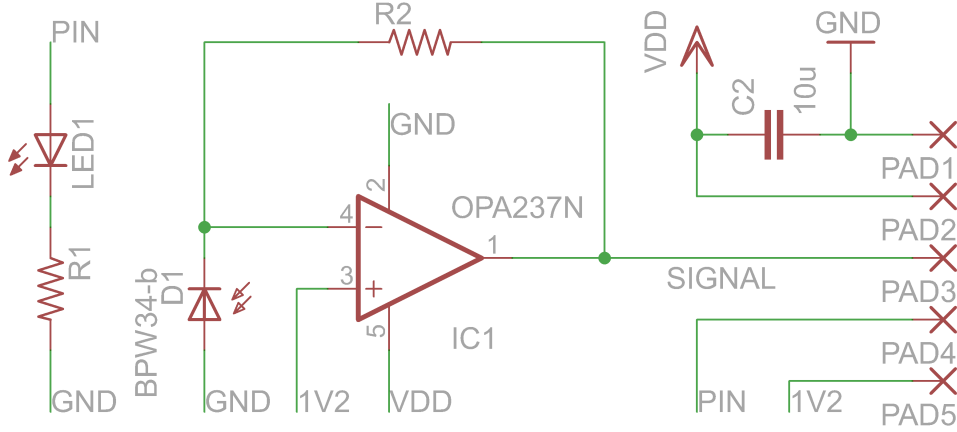


Figure 4.4: Schematic for Light Source PCB.

In the above schematic the LED is connected to a digital pin on the microcontroller. This pin's output is pulse-width modulated (PWM) signal which will be responsible for making the LED blink at a certain frequency and duty cycle. In the emission part, it also has a resistor,  $R1$ , to control the current passing through the diode. According to the datasheet of the LED (VAOL-3EUVOY4) from VCC, for a 18mA current passing through the LED, the forward voltage is of, more or less, 3.5V. The value of 18mA was chosen because it is the typical safe output of digital pins in the microcontroller. With this, the voltage across the resistor's terminals will be of  $5V - 3.5V = 1.5V$ . Using Ohm's Law the following is obtained:

$$R = \frac{U}{I} \Rightarrow R = \frac{1.5V}{0.018A} = 83.3(3)\Omega \Leftrightarrow R \approx 80\Omega \quad (4.1)$$

When the LED is turned on, the photodiode coupled to it will produce a current across its terminals directly proportional to the optical power outputted by the LED. This current signal is then converted into an amplified voltage signal using an operational amplifier in transimpedance mode. Using the configuration in Figure 4.4 with a rail-to-rail amplifier, the output signal for referencing will vary between 1.2V and VDD. The gain of the amplifier is set by the resistor  $R2$ . Using an ammeter to measure the output current of the photodiode according to the LED's previous configuration, the resistor  $R2$  can be chosen for an output transimpedance signal of 4V in average when the LED is on. this value of 4V allows for



a good monitoring range of the optical power. Through circuit analysis, and the usage of Ohm's Law, the equation for this resistor is:

$$R = \frac{U}{I} \Rightarrow \frac{V_{OUT} - V_{IN-}}{I_{PD}} = \frac{4 - 1.2}{I_{PD}} = \frac{2.8}{I_{PD}}[\Omega] \quad (4.2)$$

To note that the photodiode used is a BPW34-b by OSRAM where the b stands for *blue enhanced*, meaning it has more sensibility in the blue region of the electromagnetic spectrum, which is where the chosen photodiode operates, comparing to most photodiodes on the market.

### 4.1.2 Emitting Fluorescence

As said before, the main component of the used films is perylene, chosen for its fluorescent properties and, more importantly, its quenching in fluorescence in the presence of nitro compounds. Figure 4.5 is a photograph of the used films. Several techniques were used in order to obtain these samples, like: spin-coating, which consists of dropping the film's liquid solution onto a rotating base in order to obtain a very thin film(center); knife-coating, that is essentially a very precise knife-like machine to spread evenly the liquid solution across the base(right); or simply a controlled drop onto the glass(left). Even though there were good results with these techniques, another technique called microprinting can be tested and will possibly have better results, according to a partner project. In this thesis this technique was not used due to lack of time as it was not possible to make the films in time and it would probably lead to some adjustments in the optical chamber. As base for the the final films, two different components were tested: Ethycellulose and ZEONEX-based films. The results will be discussed in another chapter. In order to increase the repeatability and make the act of changing the film in the sensor easier, the films are made on top of a little piece of glass of dimensions 12x23mm and thickness of  $0.15 \pm 0.02\text{mm}$ , made by NORMAX.



Figure 4.5: Perylene Films

### 4.1.3 Detecting Fluorescence

On the other side of the optical chamber is the board that accommodates the photodiode responsible for detecting the fluorescence. For the same reason explained in Section 4.1.1, the photodiode chosen is the BPW34-b. The circuit is based on the same technology as the reference signal, using a rail-to-rail operational amplifier as a transimpedance amplifier with a gain based on the resistor  $R$  in the equation 4.2.

As explained before, in order to get a correct reading of the fluorescent light, an optical filter was placed before the photodiode. That led to the following spectrum obtained with the spectrometer USB4000's optical fiber placed after the filter:

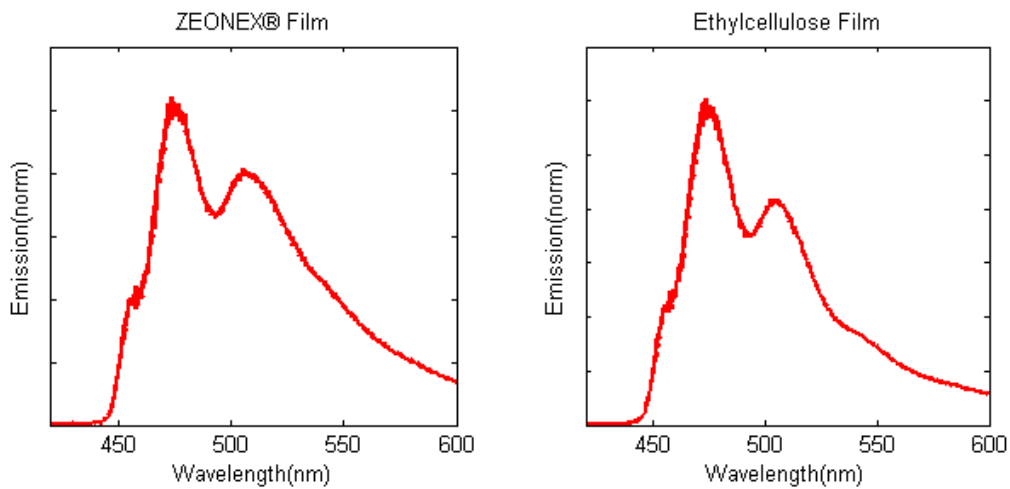


Figure 4.6: Fluorescence Spectra with films in Ethylcellulose and ZEONEX

Analyzing Figure 4.6 leads to concluding that, as expected, the film base adds little difference to the fluorescence's waveform. Some other tests regarding absolute intensity of light between these two films will be made and discussed in the next chapter.

## 4.2 Signal Conditioning

In smart sensors, usually, the objective is to take some analog signal from the world and interpret it using digital processing. For this, the analog signal has to be converted into a digital one by using an ADC. Before the ADC the signal has to be “prepared” by means of filtration, amplification and isolation. Being that the part where the analog signal from the world (light) has already been converted into an electric signal by the transducer (photodiode) and converted into a voltage signal by the transimpedance amplifier there's still some filtration before the conversion from analog to digital. This filtration is done, in

this sensor, using an instrumentation amplifier in order to get a differential type of approach between the reference and the fluorescent signals.

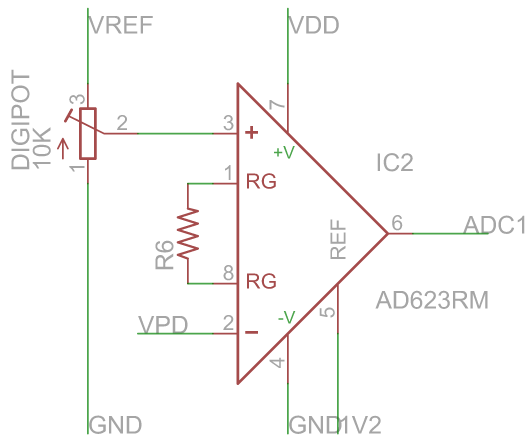


Figure 4.7: Differential approach for signal filtering

In Figure 4.7 is represented the schematic with the adopted technology. It consists of using an AD623 by Analog Devices, which is an instrumentation amplifier. This type of amplifier is known for its very low DC offset, low drift, low noise, very high open-loop gain, very high common-mode rejection ratio, and very high input impedance and is used in instrumentation also for its accuracy and stability. In this particular case it is used to subtract the fluorescence signal from the reference signal. To match the signals, a calibration algorithm was developed, using a digital potentiometer

(digiPot) to reduce the reference signal until this one is equal to the one from the fluorescence sensing photodiode. This algorithm uses the ADC to check the output of the amplifier and compare it to the 1.2V to which the amplifier is referenced, altering the value of the digiPot accordingly. This way, when there is a decrease in fluorescent light intensity, the photodiode will produce less current which will lead to a smaller signal and therefore the output signal of the instrumentation amplifier will increase:

$$V_{ADC} = (V_{REF_{bal}} - V_{Photodiode}) \times G + 1.2[V] \quad (4.3)$$

Equation 4.3 represents the formula by which the amplifier produces its output signal.  $V_{REF_{bal}}$  stands for the already balanced reference signal. The variable  $G$  is the gain of the amplifier which is selected by the resistor R6 according to what is specified in the amplifier's datasheet. This analog signal is then converted into a digital one by the ADC and processed in the microcontroller.

### 4.3 Processing

The analog part of the sensor has been covered. Going into the digital part of it, the first step was to identify what microcontroller to use. Ultimately the choice was the PIC24FV16KM202 from Microchip. It is a 28-pin microcontroller with a 16-bit architecture,

5V single supply, 32MHz PLL generated Clock Frequency and many useful modules. Some of them are used in this sensor like the Analog-to-Digital Converter, the communication interfaces like UART (Universal Asynchronous Receiver Transmitter) and  $I^2C$ , M CCP (Multiple Capture Compare Peripheral) used to generate a pulse-width modulated wave.

### 4.3.1 Interface

In terms of communication, the sensor gives the user two possibilities. Either it can communicate to an outside device through serial port or through Bluetooth. Both cases make use of the UART module inside the microcontroller.

Using TTL serial communication through the UART module, one is able to easily diffuse the wanted information through channels like the ones mentioned above. In Figure 4.8 are the examples of two modules that convert the TTL information. At the top is and FT232RL module by FTDI, which is a very common chip that allows usually a microcontroller to communicate with a computer via a USB port. This is one of the most used chips for this type of communication. On the right, the FT module is a new converter called HC-05. It is a new Chinese-made model that allows for simple communication via Bluetooth, having an integrated microcontroller that, for instance, does the pairing all by itself.



Figure 4.8: Communication Modules

### 4.3.2 Communication Protocol

Besides communication chips being very important in the versatility of a sensor, it also needs to have a user-friendly communication protocol. This protocol must meet some general requirements and sometimes, in critical situations, some encoding. In this case the protocol is a simple protocol, not compromising its robustness and functionality.

$$\langle \textit{Flag} \rangle \langle \textit{Address} \rangle \langle \textit{Length} \rangle \langle \textit{Command} \rangle \langle \textit{AdditionalData} \rangle$$

Above is represented the general structure of a message. It uses a *Flag* to signal the beginning of a message. This flag is a one byte with the hexadecimal value  $0xFF$ . In a

communication Master→Slave, the field *Address* will contain the sensor’s address whilst a communication Slave→Master will have as *Address* the code *0xFA*. This field *Address* has the length of one byte so the address value of the sensor can vary from *0* to *254* in decimal value. As default, the sensor has the address *0x10* and this value is changeable by the user. The byte in the message contains the total length in bytes of the rest of the message, *i.e.*, the sum of the fields *Command* and *Additional Data* in bytes. In the field *Command*, the user can choose a command from the list presented below in this document and each command consists of a code in hexadecimal value with the total size of one byte. Last but not least, the Part of the message *Additional Data* contains data to add to the action associated to the previous code in *Command*. Below in Table 4.1 is a list of the commands accepted by the sensor and what’s their associated action:

CODE	ACTION
0x00	Is the Sensor active?
0x10	Change Default Communication device: USB
0x11	Change Default Communication device: Bluetooth
0x12	Change Communication device: USB(once)
0x13	Change Communication Device: Bluetooth(once)
0x14	Change Device’s Address (Default:0x10)
0x15	Change USB Serial Port BaudRate (Default:19200bps)
0x20	Change Default mode of Operation: Auto
0x21	Change Default mode of Operation: Manual
0x22	Change mode of Operation: Auto(once)
0x23	Change mode of Opertaion: Manual(once)
0x30	Acquire Data and Send to Master by time(Manual Only)
0x31	Acquire Data and Send to Master by number of samples(Manual Only)

Table 4.1: Available Command Codes for Communication with the Sensor

Sometimes the code sent by the *Master* device asks for a response with some data and other times it doesn’t. When it does the structure of the message is similar the one above with the difference that it doesn’t have the field *Command*. Instead, it responds with the *Address* of the master, followed by the size of the data in *Length* and then the corresponding data that responds the request. When the message doesn’t require an answer, the devices

will only send an acknowledgement(ACK) message to let the other device know the message was received and the proper action was taken. This ACK message will have no command nor data so *Length* will be 0 and it will be of the following format:

$$\langle Flag \rangle \langle Address \rangle \langle 0 \rangle$$

Below is a list of data that can follow every command code listed above in Table 4.1. The options for the manual mode of operation consist of telling the sensor either for how long it is to be acquiring data or how many samples it has to acquire in total, specifying in both cases what is the wanted frequency in terms of samples per second. In the case of the address, it is not possible to choose the 0xFA address because this is the address that signals a communication Slave→Master.

LENGTH(max)	CODE	DATA
0x01	0x00	NULL
0x01	0x10	NULL
0x01	0x11	NULL
0x01	0x12	NULL
0x01	0x13	NULL
0x02	0x14	[0x00..0xF9]; [0xFB..0xFF]
0x02	0x15	48; 96; 192
0x01	0x20	NULL
0x01	0x21	NULL
0x01	0x22	NULL
0x01	0x23	NULL
0x03	0x30	Time( $\times 10$ [s]); Frequency[samps/10[s]] [0x00..0xFF]; [0x00..0xFF]
0x03	0x31	Number of Samples; Frequency[samps/10[s]] [0x00..0xFF]; [0x00..0xFF]

Table 4.2: Data available for each Command of Table 4.1

## I<sup>2</sup>C Forwarding

Another feature already mentioned is the possibility to add other *I<sup>2</sup>C* compatible devices to the available bus in the sensor. Essentially the sensor is able to convert a message

from the Master device and forward it to the  $I^2C$  Bus line. Having the same structure mentioned above, if the *Address* field of the message contains its own address, the sensor reads the message and interprets it according to the tables 4.1 and 4.2. If not, then the message is automatically forwarded into the  $I^2C$  bus according to the following:

DATA	HEX Value	ACTION
'S'	0x52	$I^2C$ Bus Start Sequence
'P'	0x50	$I^2C$ Bus Stop Sequence
'R'	0x52	Read Operation
'W'	0x57	Write Operation

Table 4.3: Forwarding to  $I^2C$  codes

The commands listed above in Table 4.3 are case sensitive. Apart from this commands there is also the Repeated Start action that is issued automatically when the message contains a *Read* operation immediately after a *Write* one. If the user wants to make a *Write* operation the message *Data* field should be like:

$$\langle 'W' \rangle \langle DATA_N \rangle \langle 'W' \rangle \langle DATA_{N-1} \rangle \dots \langle 'W' \rangle \langle DATA_0 \rangle$$

It is very important that the user specifies the total size in bytes of the message in the field *Length*, or else the forwarding function will not forward the whole message. To note that, in  $I^2C$  general communication, the address contains 7 bits being the 7 MSB of the byte whereas the 8<sup>th</sup> bit is the  $READ/\overline{WRITE}$  bit and it is set automatically by the function whenever the user specifies a *Read* operation. In the case of the *Read* operation, the user must specify, after the 'R' character, how many registers he wants to read. This way, the forwarding algorithm will work its way asking for data with *ACK* signal, until the last byte is asked with a *NACK*:

$$\langle 'R' \rangle \langle Length(bytes) \rangle$$

The function will then forward the received data back to the Master device at the rate it is receiving from the  $I^2C$  Slave.

## 4.4 Power Management

An important aspect of a standalone portable sensor is power management. In this sensor, the power can be from either a USB port or a li-ion 3.7V battery. For this, there is

an integrated module (the bq2423) by Texas Instruments, which is a USB-Friendly Lithium-Ion Battery Charger and Power-Path Management IC. It allows for battery charging over USB and to automatically drain power from either the USB connection or the battery if the USB cable is not connected. Another feature of this module is the charging of the battery by phases, not compromising the battery's life.

From here, Power goes to a step-up DC-DC Converter, to produce a stable 5V signal to power most part of the circuit. There are also two other linear voltage regulators, to obtain 3.3V for the Bluetooth module and 1.2V for referencing in the analog circuits.

## 4.5 Android Application

For the purpose of testing the sensor with working with Bluetooth, an Android application was developed of which a screen shot was taken, Figure 4.9. This application was developed using Android Studio. It is a program that enables the user to communicate with the sensor in a user-friendly manner. On the first window it shows a list of the already paired devices and a button that can be toggled to choose between Automatic and Manual operations. If the sensor does not appear in this list, it is because it has not been paired yet. For this the user should use the normal way of pairing Bluetooth devices, through the Bluetooth Settings menu.

When in Manual mode, after connecting to the device, a new window appears, containing an edit box and some buttons. The user can now choose the sampling frequency by which the sensor will operate. Then, the converted signal is presented exactly as it is when it leaves the microcontroller, plotting a graph in real-time in terms of 12-bit ADC, varying from 0 to 4095.



Figure 4.9: Developed Android Application



## 4.6 Enclosure

To isolate the sensor from the outside variables, an enclosure with NEMA (National Electrical Manufacturers Association) rating 4X was chosen. NEMA is the responsible entity for defining the grades of electrical enclosures used in North America. This rating states that the enclosure must be watertight in a way that it must exclude at least 65 gallons per minute of water, from a 1 inch nozzle, delivered from a distance not less than 10 ft for 5 minutes. This rating is usually for outdoor uses such as on ship docks, and in breweries. The 'X' (as 4X) indicates additional corrosion resistance.

In this enclosure three holes had to be opened: air inlet; air outlet; USB port. However, this shall not compromise the rating specified above as the inlet and outlet are very small and well isolated, and the USB port has an IP68 rating, stating that it is dust tight and is able of sustaining an immersion of 1 meter or more (usually tested at 3 meters) depth in a liquid environment.

For the ON/OFF switch, in order to not have to drill any more holes in the enclosure, a reed switch was used, glued to the inside of the enclosure, while a rotary 3D-printed button with a neodymium magnet in the middle of it, was glued to the outside, aligned with the first. This button rotates 90 degrees so that when in ON position, the magnetic field will be aligned with the reeds, making contact and powering up the circuit. When in OFF position, the reeds will be in open-circuit.



Figure 4.10: Overview of the final product



# Chapter 5

## Experimental Results

In 1999, a group of the US Army Corps of Engineers, conducted a detailed experiment to investigate the qualitative and quantitative effects of soil barriers at various temperatures on the vapor signature from buried military grade TNT [21]. They buried several quantities of military-grade TNT beneath different types of soils, analyzing the presence and quantity of some nitro compounds' vapors regarding the type of soil and, also some other environmental variables like temperature and moisture. Their experiments concludes that the concentration of this types of vapor vary greatly with temperature and humidity, and, as it was foreseeable, the longer the TNT is in the ground the higher the concentration of vapors above ground. In terms of temperature, by analyzing their tables, the hotter higher concentration of vapors, as with negative temperatures ( $-12^{\circ}\text{C}$ ), the vapors are almost untraceable. The percentage of moisture is very important as the higher concentrations were found for a moisture of 2.1%, with lower concentrations for the other two cases tested: dry air; 3.1%. For the type of soil, the tests conducted involved clay, silt and sand, where the latter showed the higher intensity of vapors. The major compounds found when analyzing the vapors through chromatography corresponded to 2,4-DNT, 1,3-DNB, 1,2-DNB, 2,3,6-TNT, and 2,4,6-TNT. For a temperature of  $23^{\circ}\text{C}$ , the concentrations of all these compounds were between the range of, roughly, 1 and  $300 \text{ pg/mL}(\times 10^{-12})$ .

As the detection of the vapors released by the explosives is not an easy task, several countries have been testing the addition to the explosives of a tagging agent. This compounds are called Explosive Taggants and can serve mainly three purposes: Detection taggants, Identification taggants and brand protection taggants. While the last one is self-explanatory, being used primarily to fight against counterfeiting, the first and second ones can be confused. The Detection taggant's purpose is to make easier the identification of

the explosive prior to its detonation, while the Identification taggant is supposed to survive detonation for post detonation identification. Between some other agents, 2,3-dimethyl-2,3-dinitrobutane (DMNB) has been internationally accepted as an additive for the purpose of marking explosives as detection taggant, as it has desired vapor pressure for reliable detection and is compatible with known explosive formulations, not altering their explosive properties [22]. It would be interesting to test the compatibility of the sensor in detecting this type tag as well. Since it also has got nitro compounds in its composition, fluorescence quenching should happen in the presence of such vapors. In terms of concentration above ground on top of the explosive, for the concentrations normally present in the explosive, it is similar to the one shown by TNT, ranging from 100 to 400 pg/mL [23].

In order to replicate these conditions to test the sensor which is the subject of this dissertation, two solutions were prepared. The first one is a solution of 2,3-dinitrobenzene (DNB), with chemical composition  $C_6H_4N_2O_4$ , while the second one is of 2,3-dimethyl-2,3-dinitrobutane (DMNB), with chemical formula  $C_6H_{12}N_2O_4$ , both of them diluted in toluene. For the DNB solution, with a molar mass of 168.11 g/mol, first a solution with a concentration of  $3.21 \times 10^{-4}M$  for a mass of 5.54 mg in 10mL of toluene was obtained. Then a  $625\mu L$  sample was extracted from this solution and added into a solution of 100 mL of toluene, giving a final concentration of  $2 \times 10^{-6}M$  which translates into  $336.22 \times 10^{-6}g/L$ .

For the DMNB solution, with a molar mass of 176.17 g/mol, first a solution with a concentration of  $1.69 \times 10^{-3}M$  for a mass of 2.98 mg in 10mL of toluene was obtained. Then a  $120\mu L$  sample was extracted from this solution and added into a solution of 100 mL of toluene, giving a final concentration of  $2.03 \times 10^{-6}M$  which translates into  $357.63 \times 10^{-6}g/L$ .

As explained before, the higher the number of nitro compounds in the vapors, the higher the quenching. With that said, reminding that TNT has three nitro compounds in its structure while DNB has only two, if detection of vapors of DNB is possible, detection of TNT vapors will most certainly be possible with the same setup. Because of security reasons, TNT was not possible to obtain for this experiment. The concentrations obtained above in



Figure 5.1: Prepared solutions of DNB and DMNB

the solutions shown in Figure 5.1 are a good starting point for what was just explained and because the concentration can still be lowered with the use of flow mass controllers before the inlet of the camera, allowing a controlled mixture between pure and impure air, where the impure air is the air contaminated with vapors from the solutions.

## 5.1 Testing Table

As explained before, to test the sensitivity of the developed sensor, two mass flow controllers were used to control a mixture of pure and impure air going through the sampling chamber. These controllers are from Bronkhorst, model F-201CV, from the family EL-FLOW, presenting a maximum flow of 75mL/min, and being controllable either from RS-232 or an analog input from 0-5V. In this case, the control was made in open-loop through the analog input, due to the fact that, in this state the sensor doesn't have enough precision to justify a closed loop control of the air flow. A simple PIC-based program was used to make this control signal. This program allowed the user to send an 8-bit value through RS-232. This value would then be used to control the internal Digital-to-Analog Converter module of the microcontroller, producing the desired analog signal to control the flow.

The air circuit for the calibration and testing of this sensor was then made out of two mass flow controllers with one air filter in each inlet, one going directly into a T-junction and another going first through the contaminated solution and then to the T-junction. The mixture then enters the sampling chamber. The outlet of the chamber is connected to a pump that is pushing the air through. The pump is at the end of the air circuit so that it does not contaminate the air going into the chamber.

## 5.2 Testing Processes

Before testing the sensor with variations in concentration by using the mass flow controllers to modify the air mixture, simple tests with just the pump pushing contaminated air were made to see if the sensor is actually sensitive enough to detect the vapors with this



Figure 5.2: Mass Flow Meter/Controller

concentration of dinitrobenzene. The results of this test, as well as the results of tests using the full air circuit are explained, shown and discussed in the following subsections. For each test it was made a comparison between the films made with ZEONEX and Ethylcellulose as well as discussing the methods of deposition of the film: knife-coating and spin-coating. For the knife-coating data, two different films of ZEONEX based perylene film were used, as well as the Ethylcellulose one. Only one of each was used for the spin coating tests.

To note that all the below graphics were obtained by processing in MATLAB the data sets acquired through the developed Android Application, via a Bluetooth connection. The sampling rate in all data sets was 10 [samples/s]. The amplifiers' gains were maintained throughout the tests.

### 5.2.1 Test1 - Maximum Impurity

This test consisted in stressing the film with the dinitrobenzene vapors at the concentration values discussed above, using the pump at its nominal power rate to push air, toggling between pure air and air from the *erlenmeyer* that contained the liquid solution. The obtained data set resulted in the following graphics obtained with the help of MATLAB:

#### Knife-Coating

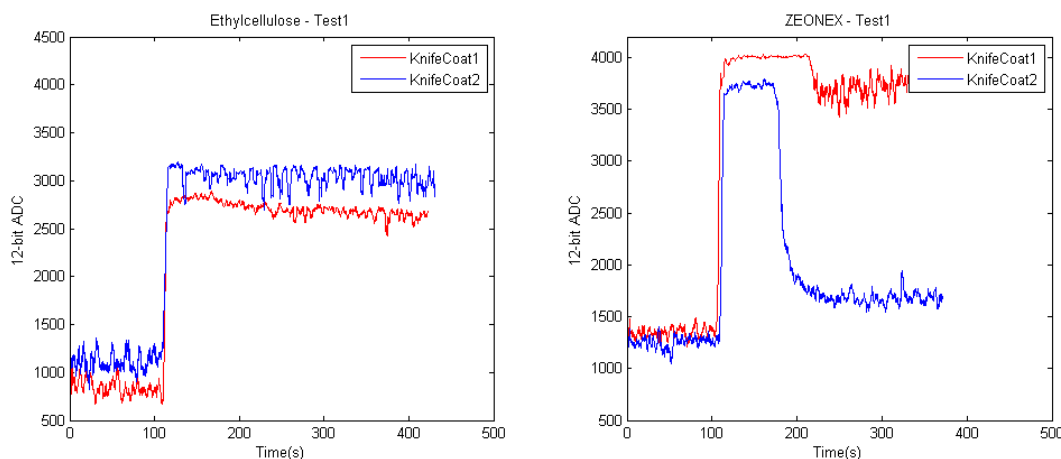


Figure 5.3: Test1 applied to ZEONEX and Ethylcellulose knife-coated films

By looking at the above, Figure 5.3, several conclusions can be taken regarding the differences between the films based in ZEONEX and Ethylcellulose. The first thing to be noticed is the difference in the response when the change impure-to-pure air is applied between them. While the Ethylcellulose based film doesn't return to the initial state after

being in the presence of dinitrobenzene vapors, the ZEONEX based one does not only seem to be more sensible to the vapor's presence, it also is much faster returning to a state near the initial one. In blue (*KnifeCoat2*), on the ZEONEX side, the main stages of this test are well identifiable, while on the Ethylcellulose side, only one stage is distinguishable. Still on the ZEONEX side, the *KnifeCoat1*'s signal saturates when in the presence of the nitroaromatic vapors. Another conclusion taken by observing this figure is the stability of the signal which seems to be better on the ZEONEX side.

### Spin-Coating

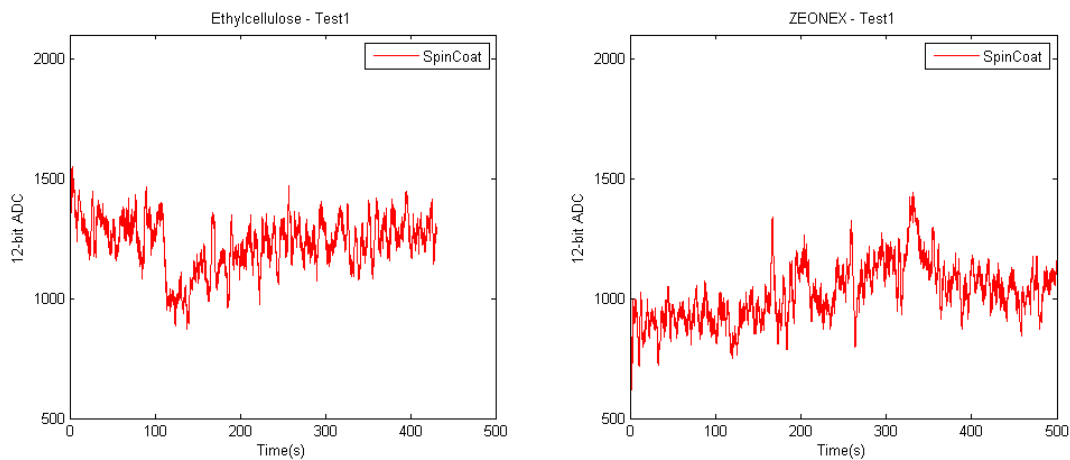


Figure 5.4: Test1 applied to ZEONEX and Ethylcellulose spin-coated films

The above Figure 5.4 shows a comparison between both types of films with a different process of deposition (Spin-Coating). The ZEONEX film appears to have a response in accordance to the one that was expected. Regarding the Ethylcellulose film, it shows an abnormal response to the vapors, that, if read in a literal way, would imply that the presence of nitroaromatic vapors would increase the intensity of fluorescence generated by the film. This suggests that probably the Ethylcellulose films have some problem.

On the ZEONEX side, although some kind of form similar to the one seen in Figure 5.3, it is much more attenuated. The signal from the films made with spin-coating is very weak when compared to the other ones. Even when tested with the spectrometer the intensity of the fluorescence generated by these films is much lower.

#### 5.2.2 Test2 - Impurity at a Controlled Flow Rate

Adding the flow controllers to the air circuit, the first step would be to do the same as in the first test, but with a much more reduced flow rate. After processing, the obtained

data set resulted in the following:

### Knife-Coating

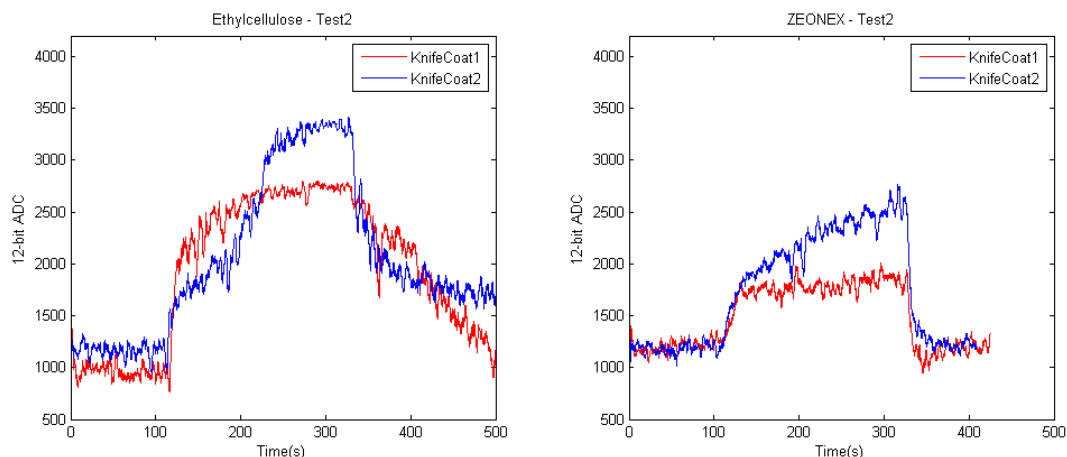


Figure 5.5: Test2 applied to ZEONEX and Ethylcellulose knife-coated films

As in Test1, there are some visible differences between the two types of films and also between different films of the same type. In both tests, it is clear that the films from which the blue graphs correspond are more sensitive to the presence of nitroaromatic vapors. Comparing both tests, it can also be concluded that the flow rate of the gas has some influence on the results. In Test1, as the flow rate was much higher than in test2, the film based in ZEONEX represented in blue, had saturated, something that does not happen with the reduced flow of Test2.

Overall, the results of this test were as expected being similar to the ones of test1 in shape, but presenting a better recovery after starting to inject uncontaminated air in the case of the Ethylcellulose. This result can be explained by the fact that the films, in their structure, are a little spongy, which allows for the vapors molecules to penetrate and infiltrate the film. Once this happens in substantial quantities, the film gets soaked, being more difficult to get cleaned up with uncontaminated air in such a way that it can return to the initial clean state. A higher flow of contaminated air results in a larger quantity of dinitrobenzene molecules penetrating the film making the film overwhelmed with dinitrobenzene.

### Spin-Coating

Once again, the spin-coated films present some abnormal results. This time, the Ethylcellulose is more coherent than the ZEONEX. In the case of the second one, it shows a surge between 120s and 200s, although the impure air was only turned off after 300s had



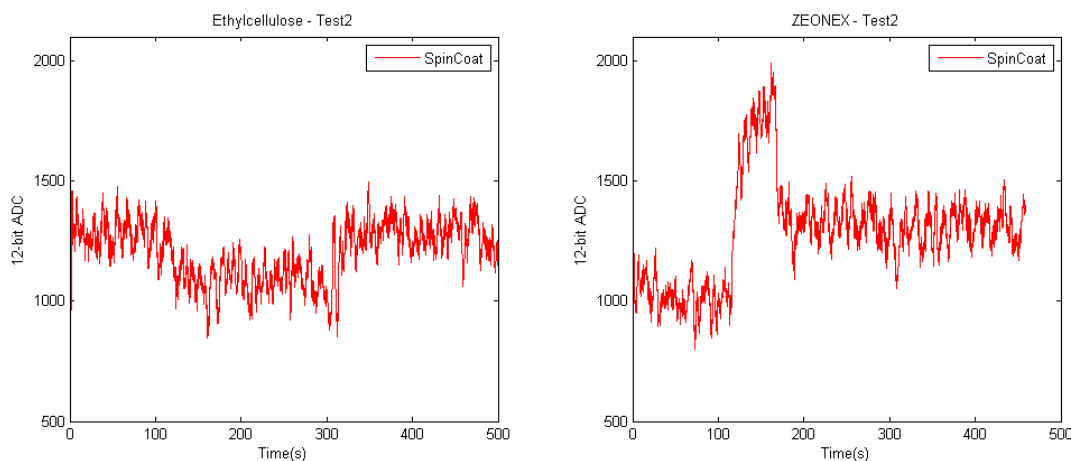


Figure 5.6: Test2 applied to ZEONEX and Ethylcellulose spin-coated films

passed. The Ethylcellulose film is coherent meaning that it is printing a signal inverted compared to what was expected. This problem will be addressed in another section further in this document.

### 5.2.3 Test3 - Mixing Pure and Impure

With the controllers in place, and connected to a PIC for controlling purposes, this test was made running a constant flow of air through the chamber for 20 minutes. Starting with uncontaminated air, from minute to minute increasing the ratio contaminated/uncontaminated by 1 step in a total of 17 steps. So, to keep a constant flow rate, while the amount of contaminated air was increased, the amount of uncontaminated air was decreased accordingly. If thinking in hexadecimal values, this 17 steps represent a range from 0x00 to 0xFF, where 0xFF stands for fully-opened and 0x00 fully-closed, when the contaminated air in the mixture is at 0x20, the uncontaminated is at 0xE0. In terms of percentage, each step corresponds to, roughly 6%, which means that for the previous example, the percentage of contaminated air would be around 12%. One minute after the mixture got to the last step (full contamination), the mass flow controllers action was inverted to get only pure air to the chamber. Another minute passed and impure air was applied again to the film, allowing nitrobenzene vapors to flow through the chamber for one more minute. Finally, pure air was injected for another minute, making the said total of 20 minutes. The results were as follows:

#### Knife-Coating

Figure 5.7 shows the results for the films that were knife-coated, when stressed by the process described above, in Section 5.2.3. As said before, when comparing Test1 and Test2,

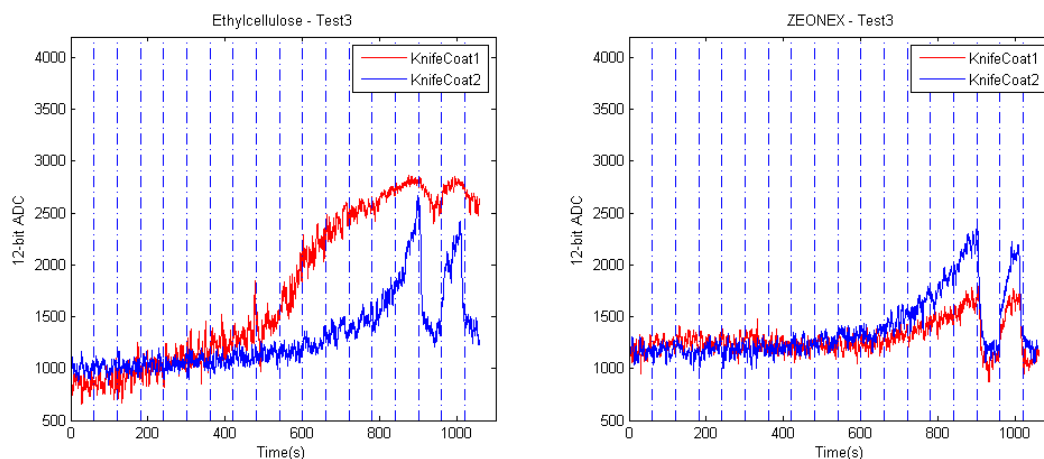


Figure 5.7: Test3 applied to ZEONEX and Ethylcellulose knife-coated films

it was concluded that the flow of the gas is of importance. Here, with this figure, the same think can be reinforced, as the signal provided by the sensor when it was supposed to be detecting dinitrobenzene vapors, continues to be attenuated when compared to the signal of Test1 (Figure 5.3), where the flow of the gas was much more intense.

Excluding the Ethylcellulose - KnifeCoat1, all the other data sets present a similar shape. This is the shape that was expected taking into account all the research done previous to this work. One other thing that has been concluded in other works is that all the films have limitations in terms of repeatability. In the State of the Art analysis (Chapter 2), it is mentioned that one sensor used a laser beam to excite the molecules in the film and this laser would burn the film, making it unusable over time. Another thing is the exposure to nitrobenzene. Altering the properties of the films, these vapors make it very difficult for them to produce the same fluorescent intensity as before the exposure. Calibration over time can, and is in the sensor, a work around this problem, so there is a decay, but the reference signal stays around the same value. However, the signal becomes so weak that even with great amplification like the one used in this sensor, the differences between having or not contaminated air in the film turn into almost nothing. Getting back to the figure, in red we see an accentuated decay of fluorescence in an almost logarithmic shape, tending to stabilize at the final steps, recovering just a little bit when clean air is applied. The reason for this is what was just explained before, being that this film was used several times since the moment when tests began to be made on the developed acquisition board.

Another thing that can be reinforced under the conditions of this test, and specifically comparing the data sets present in Figure 5.7, is the more stable and faster way that ZEONEX-based films recover from a full contamination to a no contamination state.

## Spin-Coating

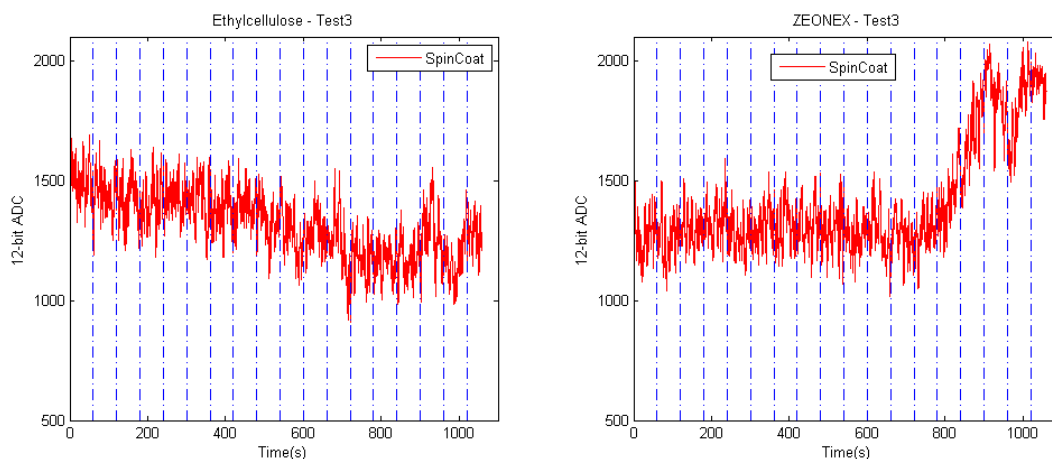


Figure 5.8: Test3 applied to ZEONEX and Ethylcellulose spin-coated films

Once again, the film of which the polymeric base is Ethylcellulose gives out a data set inverted compared to what was expected, and what was retrieved with the knife-coated films for the same test. A deeper analysis may suggest that what is shown in the figure is not related to the fluorescence emitted by the excited film, but to the light provided by the excitation source. There is some part of this light that goes through the optical filter and may surpass the intensity of the fluorescence, even though the photodiode is more sensitive to the wavelength of the fluorescence than to the wavelength of excitation source. The film absorbs some of the excitation light so in terms of transmission it can be seen as a filter. To emit less fluorescence it absorbs less light, transmitting more light and vice-versa. With that said, in the presence of dinitrobenzene it transmits a higher percentage of the excitation light, therefore, the signal produced by the photodiode will be higher. Following with the configuration in Figure 4.7, this signal is being subtracted to the reference one, outputting a weaker signal at the end of the signal conditioning chain.

As for the ZEONEX-based one, the response was above expectations, presenting some good differentiation towards the last stages of the test, coherent to the knife-coated responses.

## 5.3 Response Analysis

Below, in Figure 5.9, is the result of the analysis of a data set from Test3 obtained with MATLAB:

As this data set is from the procedure described in Test3 (Section 5.2.3), there was a change in state from minute to minute, adding up more and more contamination to the mix-

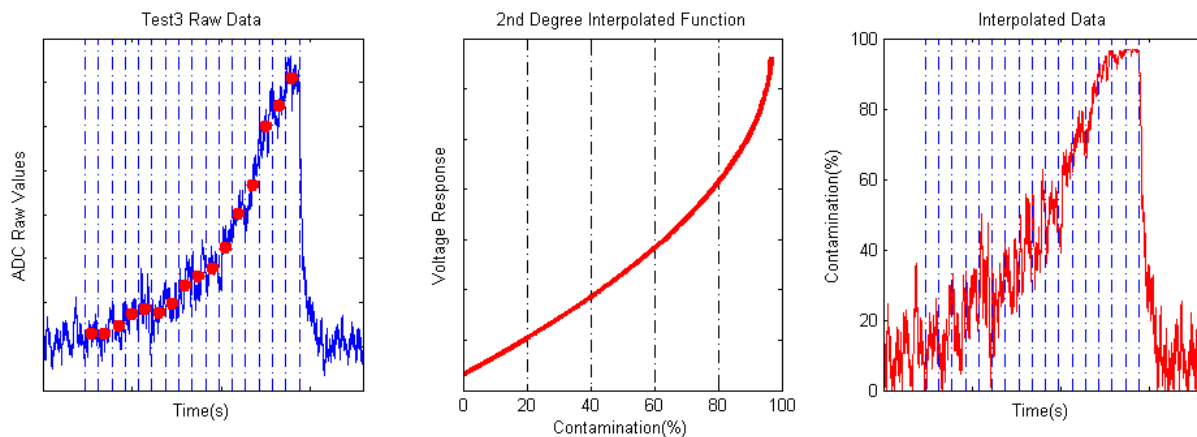


Figure 5.9: Interpolation of data set from Test3's procedure

ture going into the chamber, until it was 100% composed of vapors from the dinitrobenzene solution.

After it was acquired, the data set was divided in minutes, as each minute represents a different stage and the respective mean value of the stage calculated. With the help of the *polyfit()* MATLAB function, the data set was approximated to a polynomial function of second order, being the result as was drawn in the middle graph of the above figure. This graph was obtained by using the function *polyval()* with the coefficients that were previously calculated. This polynomial is function of the ADC values obtained with the sensor. On the other hand, the ADC values are directly related to the DC voltage signal outputted by the analog conditioning circuit which directly proportional to the inputs from the photosensitive sensors that are in terms of current. This current, as described in the photodiode's datasheet, and as with all the previous relations, is directly and linearly proportional to the optical power received. This allows and gives support to the conclusion that the response of the films in terms of decrease in intensity of fluorescence behaves exponentially in relation to the concentration of nitroaromatic vapors, specifically dinitrobenzene.

This results also prove that this sensor's method of acquiring the intensity of the fluorescence has enough sensitivity, in terms of electronics and optical conditioning, to be able to take quantitative measures and correlate them with levels of concentration of nitroaromatic vapors. The way to improve it in such a manner that it makes this possible is discussed in the Future Work, Section 6.1.

Another conclusion that can be reinforced from the acquired data sets is that the thickness of the film matters. The main problem with the spin coating is that it leaves a very thin layer of film on top of the glass. This causes the response to be, as discussed previously, much more attenuated than, for instance, with the knife-coating process, which

leaves a thicker layer of film. This response is terms of ratio between fluorescent intensity and the intensity of the excitation light.



# Chapter 6

## Conclusion

A series of objectives have been defined in Chapter 1.2. As a conclusion there shall be a comparison between what was the initial idea in terms of goals and the actual sensor's performance.

Overall the results obtained in this dissertation were in accordance with the initial expectations and proposed objectives, keeping in mind that this is a prototype for a new method of explosives detection, with a configuration not yet tested until now.

Most of the problems were related to the non-homogeneity of the films and the process of deposition of this film onto a small piece of glass. Taking into account that the manufacturing of the polymeric films was not the object of study in this dissertation, these problems were not taken into account from the beginning. Said problems can be categorized as external factors that conditioned the results presented and therefore the performance of the prototype. Still regarding the films, the results obtained in this dissertation suggest that the use of ZEONEX as the polymeric matrix of the perilene films is better than the use of Ethylcellulose.

Some other problems originated from the manufacturing of the PCB. It was made, as said at the beginning of this document, using an LPKF milling machine. This presented

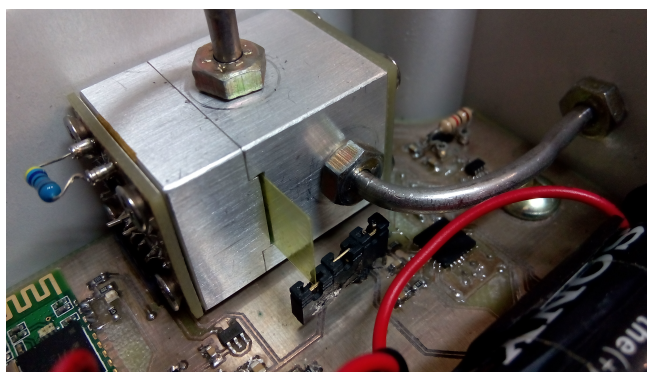


Figure 6.1: Overview of the final product

some other challenges as this process is very good for quickly making small prototypes but it is very time consuming when used to mill bigger PCB's like the main one in this sensor. After the milling process, the soldering of all the components and vias is also more time consuming than with a professionally manufactured board, in part because of the absence of a solder mask and because the vias, instead of all at once in an electro-chemical process, are soldered with a wire one by one.

Having discussed the problems, there were many other things that went well. One of the goals described in the Objectives Section was to keep the electronics simple. This was successfully achieved not compromising the sensor's abilities and performance.

It is portable, it detects the nitroaromatic compounds, it uses fluorescent films to do so, it proves the possibility of correlating fluorescence intensity with nitroaromatic concentration, it is not too complex which makes it not too expensive to build, it is a solution. In conclusion, the objectives were maintained and respected throughout the project, turning them into results, which makes the project successful.

## 6.1 Future Work

Although this version of the sensor works as expected in terms of detecting the presence of Nitrobenzene vapors, in electronics there are always some things that, at the end could be changed to make it better.

A problem that occurred regarding the films used was the lack of repeatability between different ones, due to the processes of deposition. By using microprinting, we could make sure that the films would be very similar in terms of dimensions and homogeneity. The non-homogeneity of films resulted on having to calibrate the gains of the amplifiers in the analog conditioning circuit for almost each time we tested a different film.

Now that this sensor works and can be seen as a good proof of concept, in terms of future work, there are some aspects of it that could be changed for better accuracy and precision. As referenced above in this document, there is another method of constructing the sensitive films that delivers a much more precise and homogeneous film, which is through microprinting. This method was not used because it was not possible at the time of the development of this sensor. It allows for a different approach, maybe using a focused laser with a much smaller sampling chamber. It solves problems of homogeneity making it possible to change between filter with just a simple calibration, without having to change the gains of the amplifiers, making the overall solution a better sensor.



# Bibliography

- [1] L. . C. M. Monitor, 2014. [Online]. Available: <http://www.the-monitor.org/en-gb/media/additional-resources/maps-and-tables.aspx>
- [2] M. Pokrzywnicka, R. Koncki, and Łukasz Tymecki, “A concept of dual optical detection using three light emitting diodes,” *Talanta*, 2010.
- [3] R. von Wandruszka, M. Pollard, and M. Spinner, “Construction and evaluation of a fluorescent sensor for the detection of high explosives,” *Analytical Letters*, 2013.
- [4] M. O’Toole and D. Diamond, “Absorbance based light emitting diode optical sensors and sensing devices,” *Sensors*, 2008.
- [5] R. Schroeder, Friedhelm; Prien, “Oxygen sensors.” [Online]. Available: [http://www.coastalwiki.org/wiki/Oxygen\\_sensors](http://www.coastalwiki.org/wiki/Oxygen_sensors)
- [6] T. Neves, L. Marques, L. Martelo, and H. Burrows, “Conjugated polymer-based explosives sensor: Progresses in the design of a handheld device,” 2014.
- [7] FLIR<sup>®</sup>. [Online]. Available: [http://www.flir.com/uploadedFiles/flirGS/Threat\\_Detection/Explosives\\_Detection/Products/Fido\\_X3\\_Explosives\\_Detector/Datasheet%20Fido%20X3%2009012015%20EN.pdf](http://www.flir.com/uploadedFiles/flirGS/Threat_Detection/Explosives_Detection/Products/Fido_X3_Explosives_Detector/Datasheet%20Fido%20X3%2009012015%20EN.pdf)
- [8] R.-C. A. Fuh, “Optical absorption measurement of perylene,” June 1995. [Online]. Available: <http://omlc.org/spectra/PhotochemCAD/html/023.html>
- [9] E. O. Inc. [Online]. Available: <http://www.edmundoptics.com/optics/optical-filters/longpass-edge-filters/dichroic-laser-beam-combiners/86382/>
- [10] U. Nations. [Online]. Available: [http://www.un.org/Depts/mine/UNDocs/ban\\_trty.htm](http://www.un.org/Depts/mine/UNDocs/ban_trty.htm)

- [11] B. Ki-moon. [Online]. Available: [http://www.un.org/en/events/mineawarenessday/2015/sg\\_message.shtml](http://www.un.org/en/events/mineawarenessday/2015/sg_message.shtml)
- [12] C. Aker, C. Cumming, M. Fisher, M. Fox, M. IaGrone, D. Reust, M. Rockley, and E. Towers, "Vapor sensing instruments for ultra trace chemical detection," 2008, uS Patent 7,419,636.
- [13] H. Favre and W. Powell, *Nomenclature of Organic Chemistry: IUPAC Recommendations and Preferred Names 2013*, ser. International Union of Pure and Applied Chemistry. Royal Society of Chemistry, 2013.
- [14] C. for Disease Control and Prevention(CDC), "Facts about benzene," February 2013. [Online]. Available: <http://www.bt.cdc.gov/agent/benzene/basics/facts.asp>
- [15] A. for Toxic Substances and D. Registry(ATSDR), *Toxicological Profile for Polycyclic Aromatic Hydrocarbons (PAHs)*. Atlanta, U.S.: U.S. Department of Health and Human Services, Public Health Service, August 1995.
- [16] R. C. Jaeger and T. N. Blalock, *MICROELECTRONIC Circuit Design*, 4th ed. Avenue of the Americas, New York: The McGraw-Hill Companies, In, 2011.
- [17] I. M. Fund, "World economic outlook database," October 2015. [Online]. Available: <http://www.imf.org/external/pubs/ft/weo/2015/02/>
- [18] [Online]. Available: <http://www.moorelaw.org/>
- [19] P. Mottier, *LED for Lighting Applications*. John Wiley & Sons, 2010.
- [20] F. Tavernier and M. Steyaert, *High-Speed Optical Receivers with Integrated Photodiode in Nanoscale CMOS*, ser. Analog Circuits and Signal Processing. Springer Science & Business Media, 2011.
- [21] a. T. A. R. Thomas F. Jenkins, Daniel C. Leggett, "Vapor signatures from military explosives, part 1. vapor transport from buried military-grade tnt," US Army Corps of Engineers<sup>®</sup>, Tech. Rep., 1999.
- [22] R. Sinha, H. Shekhar, A. S. Rao, and H. Singh, "Modelling of dmn content for marked plastic explosives," *Defence Science Journal*, vol. 57, no. 6, 2007.
- [23] J. Yinon, *Forensic and Environmental Detection of Explosives*. Wiley, 1999.